Diana-Elena Gratie | Bogdan Iancu | Sepinoud Azimi | Ion Petre

Quantitative model refinement in four different frameworks, with applications to the heat shock response

Turku Centre *for* Computer Science

TUCS Technical Report
No 1067, February 2013

Quantitative model refinement in four different frameworks, with applications to the heat shock response

Diana-Elena Gratie
Computational Biomodelling Laboratory, Åbo Akademi University and Turku Centre for Computer Science, FI-20520 Turku, Finland
dgratie@abo.fi

Bogdan Iancu
Computational Biomodelling Laboratory, Åbo Akademi University and Turku Centre for Computer Science, FI-20520 Turku, Finland
biancu@abo.fi

Sepinoud Azimi
Computational Biomodelling Laboratory, Åbo Akademi University and Turku Centre for Computer Science, FI-20520 Turku, Finland
sazimi@abo.fi

Ion Petre
Computational Biomodelling Laboratory, Åbo Akademi University and Turku Centre for Computer Science, FI-20520 Turku, Finland
ipetre@abo.fi

TUCS Technical Report
No 1067, February 2013

Abstract

When compiling a biological model, one often starts with an abstract representation, that is subsequently refined through several consecutive steps to incorporate more details regarding various reactants and/or reactions. To avoid the computationally expensive refitting of the model after each refinement step, the new parameters should be set so that the numerical behavior of the initial model is preserved. The iterative process of adding details to a model while preserving its numerical behavior is called *quantitative model refinement*, and it has been previously discussed for ODE-based models and for *kappa*-based models. In this paper, we investigate and compare this approach in four modeling frameworks: ordinary differential equations, rule-based modeling, Petri nets and guarded command languages. As case study we use a model for the eukaryotic heat shock response that we refine to include the acetylation of one molecule. We discuss how to perform the refinement in each of these frameworks in order to avoid the combinatorial state explosion of the refined model. We conclude that Bionetgen (and rule-based modeling in general) is well-suited for a compact representation of the refined model, Petri nets offer a good solution through the use of colors, while the PRISM refined model may be much larger than the basic model.

Keywords: Quantitative model refinement, heat shock response, acetylation, rule-based modeling, Petri nets, model checking.

TUCS Laboratory
Computational Biomodeling Laboratory

1 Introduction

Systems biology aims to holistically characterize highly complex biological systems. A hierarchical system-level representation is very adequate in this context. Formal frameworks turn out to be fundamental in the effort of understanding the behavior of such complex systems, see [30, 20]. Some argue even that this might be a crucial path that biology could take in order for it to progress [2]. At the core of this approach lies an abstraction of the biological phenomena, eventually materialized into a model derived through an iterative process of model building that consists in a series of steps such as: system design, model analysis, hypothesis generation, hypothesis testing, experimental verification and model refinement, see [30]. Some of these abstractions need to be refined to incorporate more details. Reiterating the whole model development process is time-consuming and computationally intensive. This is why a formal method of refining a model when starting from an existing higher-level abstraction is needed.

We focus in this paper on the implementation of the model refinement step from the model development process introduced above. Within the model development process, we examine *data refinement* through four different frameworks – *ODEs, rule-based modeling, Petri nets* and *guarded command languages* – and discuss their capabilities for the efficient construction of a refined model. For rule-based modeling we use the Bionetgen framework and RuleBender, for Petri nets we chose Snoopy and Charlie as modeling tools, while for modeling with guarded command languages we used PRISM. In the case of data refinement, as proposed in [7] and [18], the model is refined by replacing one species in the model with several of its variants, called subspecies. This type of refinement is adequate for representing post-translational modifications of proteins, e.g., acetylation, phosphorylation, etc. Given a protein P, one can indicate its state regarding post-translational modifications by replacing it with its variants. This substitution also implies a refinement of all complexes involving protein P and of all reactions involving either P or any such complex, see [18]. This might induce a combinatorial state explosion of the refined model, as in the case of ODE-based models, see [18]. The main question we are answering is whether one can avoid this problem in the other three frameworks we investigate in this paper and build a compact representation of the refined model.

We consider as a case study for our analysis the heat shock response mechanism, as described in [29] and [18]. Throughout the paper, the model in [29] will be referred to as the *basic* heat shock response model, while the model in [18] will be referred to as the *refined model*.

The paper is organised as follows: we start with a short description of the biological process of heat shock response in Section 2, together with the reaction-based model proposed in [29]. We also present here the acetylation of proteins and its implications with regards to the heat shock response. We detail the mechanism of quantitative model refinement in Section 3, focusing in Section 4 on the refine-

ment of ODE-based models. In Section 5, we introduce a Petri net implementation of the heat shock response and we present its refinement using colored Petri nets. In Section 6, we present a rule-based implementation of the heat shock response and its corresponding refinement. Section 7 comprises an implementation of the basic and the refined model for the heat shock response in PRISM. All models developed in this paper can be downloaded at `http://goo.gl/LJLIxk`.

2 The heat shock response (HSR)

The eukaryotic *heat shock response* is a highly conserved bio-regulatory network that controls cellular function impairment produced by protein misfolding as a result of high temperatures. Elevated temperatures have proteotoxic effects on proteins, inducing protein misfolding and leading to the formation of large aggregates that thereafter trigger apoptosis (controlled cell death). Cell survival is promoted by a defense mechanism, which consists in restoring protein homeostasis by augmenting the level of molecular chaperones, see [33, 37].

We consider the basic molecular model for the eukaryotic heat shock response proposed in [29]. *Heat shock proteins* (hsp's) play a key role in the heat shock response mechanism by chaperoning the *misfolded proteins* (mfp's). Due to their affinity to mfp's, hsp's form hsp: mfp complexes and help the misfolded proteins refold. The heat shock response is regulated by the transactivation of the hsp-encoding genes. In eukaryotes, some specific proteins, called *heat shock factors* (hsf's), promote gene transcription. In the absence of environmental stressors, heat shock factors are predominantly found in a monomeric state, extensively bound to heat shock proteins. Raising the level of temperature causes the correctly folded proteins (prot) to misfold and hsp: hsf complexes to break down. This switches on the heat shock response by releasing hsf's, which quickly reach a DNA binding competent state, see [29, 35].

Heat stress induces dimerization (hsf_2) and, subsequently, trimerization (hsf_3) of hsf's, enabling the binding of the hsf trimers to the promoter site of the hsp-encoding gene, called *heat shock element* (hse). Subsequently, DNA binding triggers the transcription and translation of the hsp-encoding gene, inducing hsp synthesis, see [29, 33]. Once the level of heat shock proteins is sufficiently elevated for the cell to withstand thermal stress, hsp synthesis is turned off. Heat shock proteins sequestrate heat shock factors and break hsf dimers and trimers, constituting hsp: hsf complexes.

The molecular reactions constituting the model are listed in Table 1.

The kinetic rate constants and initial values of reactants were estimated in [29] to satisfy the following conditions:

(i) the system is in a steady state for a temperature of $37°C$ since the model should not indicate any response in the absence of the heat shock, i.e., at $37°C$;

Table 1: The molecular model for the eukaryotic heat shock response proposed in [29]

Reaction	Description
$2\,\mathsf{hsf} \rightleftarrows \mathsf{hsf}_2$	Dimerization
$\mathsf{hsf} + \mathsf{hsf}_2 \rightleftarrows \mathsf{hsf}_3$	Trimerization
$\mathsf{hsf}_3 + \mathsf{hse} \rightleftarrows \mathsf{hsf}_3\mathsf{:\,hse}$	DNA binding
$\mathsf{hsf}_3\mathsf{:\,hse} \rightarrow \mathsf{hsf}_3\mathsf{:\,hse} + \mathsf{hsp}$	hsp synthesis
$\mathsf{hsp} + \mathsf{hsf} \rightleftarrows \mathsf{hsp}\mathsf{:\,hsf}$	hsf sequestration
$\mathsf{hsp} + \mathsf{hsf}_2 \rightarrow \mathsf{hsp}\mathsf{:\,hsf} + \mathsf{hsf}$	Dimer dissipation
$\mathsf{hsp} + \mathsf{hsf}_3 \rightarrow \mathsf{hsp}\mathsf{:\,hsf} + 2\,\mathsf{hsf}$	Trimer dissipation
$\mathsf{hsp} + \mathsf{hsf}_3\mathsf{:\,hse} \rightarrow \mathsf{hsp}\mathsf{:\,hsf} + 2\,\mathsf{hsf} + \mathsf{hse}$	DNA unbinding
$\mathsf{hsp} \rightarrow \emptyset$	hsp degradation
$\mathsf{prot} \rightarrow \mathsf{mfp}$	Protein misfolding
$\mathsf{hsp} + \mathsf{mfp} \rightleftarrows \mathsf{hsp}\mathsf{:\,mfp}$	mfp sequestration
$\mathsf{hsp}\mathsf{:\,mfp} \rightarrow \mathsf{hsp} + \mathsf{prot}$	Protein refolding

(ii) the numerical predictions of the model for $[\mathsf{hsf}_3\mathsf{:\,hse}](t)$ should confirm the experimental data from [21], for a temperature of $42^{\circ}C$;

(iii) the numerical prediction of the model for $[\mathsf{hsp}](t)$ should be in accordance with the data attained in [29] , for a temperature of $42^{\circ}C$.

The numerical setup of the basic model (in terms of initial concentrations and kinetic constants) can be found in [29].

We discuss in the following the acetylation details of the heat shock factors and their role in the heat shock response. Heat shock factors (hsf's) are determining factors in cell survival, protecting the cell from environmental stressors associated with protein damage, such as protein misfolding. Acetylation has been shown to have an extensive influence in regulating the heat shock response, we refer the reader to [38]. Protein acetylation is the process of substituting an acetyl group for a hydrogen atom in a chemical compound. It can occur either at the α-amino group of the N-terminal (N-terminal acetylation) or at the ϵ-amino group on lysine residues (lysine acetylation), see [11, 6, 17].

N-terminal acetylation is irreversible - once acetylated, proteins maintain their acetylation status until decomposition. Despite having been extensively studied in the past decades, the functional significance of N-terminal acetylation is not entirely understood. However, new studies have shown that it plays a key role in cell survival, see [1].

Lysine acetylation is a highly conserved post-translational modification in eukaryotes, it attenuates DNA binding activity by neutralizing the positive charge of histones and, thus, regulates gene expression, see [6].

3 Quantitative model refinement

Quantitative model refinement was investigated in [28, 8] regarding rule based modeling and applied to two ampler ODE-based models in [27, 18].

3.1 Quantitative model refinement

An important role in the model development cycle discussed in Section 1 is played by *model refinement*. A reaction-based model can be refined to incorporate more information regarding its reactants and/or reactions. There are two types of refinement, either of the *data* (data refinement) or of the *reactions* (process refinement). In this study, we focus on the first refinement type. Considering that one's interest lies especially on data, a species in a model could be refined by replacing it with several of its subspecies, a routine called *data refinement*. Several reasons underlie the choice of data refinement as modus operandi: expressing various internal states or attributes of some reactants of interest, exploring the behavioral fluctuations manifested in the subspecies of a particular species, etc. When the interest is focused on reactions, the model can be refined by replacing a collective reaction, accounting for a specific process, by a set of reactions depicting the transitional steps of the process. The last type of refinement is called *process refinement*, see [18].

The notion of *quantitative model refinement* has been previously addressed in systems biology in the context of rule based modelling, see [28, 8, 12, 9]. The rule based modelling framework embodies the concept of *data refinement*, implementing agent resolution as a fundamental constituent, [12]. The key refinement method in this context is rule refinement, an approach that requires the refinement of the set of rules ensuring the preservation of the dynamic behavior of the system, see [28].

We give in the following a formal definition of quantitative model refinement for reaction-based models. Consider a model M, comprising *species* $\Sigma_M = \{A_1, \ldots, A_l, A_{l+1}, \ldots, A_m\}$ and *reactions* $R_M = \{r_1, \ldots, r_n\}$. We distinguish two types of species: *atomic* species and *complex* species; the intuition here is that complex species are composed of two or more atomic species. Without loss of generality, we denote by $\Gamma_M = \{A_1, \ldots, A_l\}$ the set of atomic species and by $\Delta_M = \{A_{l+1}, \ldots, A_m\}$ the set of the complex ones. For each complex species $C \in \{A_{l+1}, \ldots, A_m\}$ we indicate through a multiset $\sigma(C)$ its atomic components:

$$\sigma(C) = \{m_1^C A_1, \ldots, m_l^C A_l\},$$

where $m_1^C, \ldots, m_l^C \in \mathbb{N}$ and $\sum_{i=1}^{l} m_i^C \geq 2$. If $m_i^C \neq 0$, then we say that the complex species C *contains* atomic species A_i with multiplicity m_i^C. For each atomic species $A_i, 1 \leq i \leq l$, we denote by $\mathscr{C}_M(A_i)$ the set of complex species containing A_i:

$$\mathscr{C}_M(A_i) = \{C \in \{A_{l+1}, \ldots, A_m\} \mid m_i^C \neq 0\}.$$

Each reaction r can be written as a rewriting rule of the form

$$r \ : \ s_1A_1 + \ldots + s_mA_m \xrightarrow{k_r} s'_1A_1 + \ldots + s'_mA_m, \tag{1}$$

where $s_1, \ldots, s_m, s'_1, \ldots, s'_m \in \mathbb{N}$ are the *stoichiometric coefficients* of r and $k_r \geq 0$ is the *kinetic rate constant* of reaction r.

The goal of the refinement is to introduce details into the model, in the form of distinguishing several subspecies of a given species. The distinction between the subspecies is very often drawn by post-translational modifications such as acetylation, phosphorylation, sumoylation, etc., but it could also account for different possible types of a particular trait (e.g. fur color of animals in a breeding experiment).

We are only concerned in this paper with refining one atomic species at a time. Without loss of generality, assume that the species to be refined is A_1. Simultaneously with refining A_1, all complexes in $\mathscr{C}_M(A_1)$ should also be refined. Each species $X \in \Sigma_M \setminus \big(\{A_1\} \cup \mathscr{C}_M(A_1)\big)$ that is not subject to refinement will be replaced in the *refined model* M_R with new species X^R.

If A_1 is replaced in the refined model with $\{A_1^1, \ldots, A_1^\rho\}$, then a species $C \in \mathscr{C}_M(A_1)$ with $\sigma(C) = \{m_1A_1, \ldots, m_lA_l\}$ is replaced by $\mathscr{R}(C) = \{C^1, \ldots, C^\mu\}$, where $\mu = \left(\!\!\binom{\rho}{m_1}\!\!\right)$ is the *multiset coefficient*, ρ *multichoose* m_1. Each refined species C^i is a complex species with $\sigma(C^i)$ of the form

$$\sigma(C^i) = \{\tau_1A_1^1, \ldots, \tau_\rho A_1^\rho, m_2A_2^R, \ldots, m_lA_l^R\},$$

where $\tau_1, \ldots, \tau_\rho \in \mathbb{N}$, $\tau_1 + \cdots + \tau_\rho = m_1$.

The refined model M_R consists of atomic species $\Gamma_{M_R} = \{A_1^1, \ldots, A_1^\rho\} \cup \{A_2^R, \ldots, A_l^R\}$ and of complex species $\Delta_{M_R} = \bigcup_{C \in \mathscr{C}_M(A_1)} \mathscr{R}(C) \bigcup \{C^R \mid C \in \Delta_M \setminus \mathscr{C}_M(A_1)\}$.

Moreover, in each reaction r of M, we replace A_1 and the species in $\mathscr{C}_M(A_1)$ with their refined subspecies, in all possible combinations. If a species X to be refined into $\{X^1, \ldots, X^\nu\}$ has stoichiometric coefficient s in reaction r, then it will be replaced in the refinement of r with $s^1X^1 + \ldots + s^\nu X^\nu$, where $s^1, \ldots, s^\nu \in \mathbb{N}$, $s^1 + \ldots + s^\nu = s$. Formally, reaction r of form (1) is replaced with all possible reactions $\hat{r}$ of the form

$$\begin{aligned}
\hat{r} \ : & \big(s_1^1A_1^1 + \ldots + s_1^\rho A_1^\rho\big) + \big(s_2A_2^R + \ldots + s_lA_l^R\big) + \\
& \sum_{A_i \in \mathscr{C}_M(A_1)} \sum_{C \in \mathscr{R}(A_i)} s_{A_i}^C C + \sum_{A_i \in \Delta_M \setminus \mathscr{C}_M(A_1)} s_iA_i^R \\
\xrightarrow{k_{\hat{r}}} & \big(s_1'^1A_1^1 + \ldots + s_1'^\rho A_1^\rho\big) + \big(s'_2A_2^R + \ldots + s'_lA_l^R\big) + \\
& \sum_{A_i \in \mathscr{C}_M(A_1)} \sum_{C \in \mathscr{R}(A_i)} s'^C_{A_i} C + \sum_{A_i \in \Delta_M \setminus \mathscr{C}_M(A_1)} s'_iA_i^R,
\end{aligned}$$

where:

- $s_1^1 + \ldots + s_1^\rho = s_1,\ s_1^1, \ldots, s_1^\rho \in \mathbb{N}$;
- $s_1'^1 + \ldots + s_1'^\rho = s_1',\ s_1'^1, \ldots, s_1'^\rho \in \mathbb{N}$;
- $\sum_{C \in \mathscr{R}(A_i)} s_{A_i}^C = s_i,\ s_{A_i}^C \in \mathbb{N}, \forall A_i \in \mathscr{C}_M(A_1)$;
- $\sum_{C \in \mathscr{R}(A_i)} s_{A_i}'^C = s_i',\ s_{A_i}'^C \in \mathbb{N}, \forall A_i \in \mathscr{C}_M(A_1)$.

Model M_R is said to be a *data refinement of model* M *on variable* A_1 if and only if the following conditions are fulfilled at any time point $t \geq 0$:

$$[A_1](t) = [A_1^1](t) + \ldots + [A_1^\rho](t); \tag{2}$$

$$[A_i](t) = \sum_{C \in \mathscr{R}(A_i)} [C](t),\ \text{for all } A_i \in \mathscr{C}_M(A_1); \tag{3}$$

$$[A_i](t) = [A_i^R](t),\ \text{for all } A_i \in \Sigma_M \setminus \big(\{A_1\} \cup \mathscr{C}_M(A_1)\big). \tag{4}$$

Fulfilling these conditions depends on the numerical setup of model M_R, i.e., on the kinetic constants of its reactions (both those adopted from the basic model, as well as those newly introduced in the construction) and on the initial concentrations of its species.

3.2 Adding the acetylation details to the HSR model through data refinement

We follow here the discussion in [18]. We start from the basic model of the heat shock response, introduced in [29], where no post-translational modification of hsf is taken into account, and we refine all species and complexes that involve hsf taking into consideration one acetylation site for every hsf molecule. The aim is to refine the basic model and preserve its numerical properties. For hsf_2, hsf_3, hsf_3: hse and hsp: hsf, the refinement is performed conforming to the number of hsf constituents respectively. This leads to the following data refinement:

$$\begin{aligned}
&\mathsf{hsf} \to \{\mathsf{rhsf}, \mathsf{rhsf}^{(1)}\};\\
&\mathsf{hsf}_2 \to \{\mathsf{rhsf}_2, {\mathsf{rhsf}_2}^{(1)}, {\mathsf{rhsf}_2}^{(2)}\};\\
&\mathsf{hsf}_3 \to \{\mathsf{rhsf}_3, {\mathsf{rhsf}_3}^{(1)}, {\mathsf{rhsf}_3}^{(2)}, {\mathsf{rhsf}_3}^{(3)}\};\\
&\mathsf{hsf}_3\mathsf{:\,hse} \to \{\mathsf{rhsf}_3\mathsf{:\,rhse}, {\mathsf{rhsf}_3}^{(1)}\mathsf{:\,rhse}, {\mathsf{rhsf}_3}^{(2)}\mathsf{:\,rhse},\\
&{\mathsf{rhsf}_3}^{(3)}\mathsf{:\,rhse}\};\\
&\mathsf{hsp:\,hsf} \to \{\mathsf{rhsp:\,rhsf}, \mathsf{rhsp:\,rhsf}^{(1)}\}.
\end{aligned}$$

The refinement cycle based on the above data refinements involves substantial changes in the list of reactions. For example, the reversible reaction of dimerization $2\,\mathsf{hsf} \rightleftarrows \mathsf{hsf}_2$ in the basic model is replaced by three reactions as follows: $2\,\mathsf{rhsf} \rightleftarrows \mathsf{rhsf}_2$; $\mathsf{rhsf} + \mathsf{rhsf}^{(1)} \rightleftarrows {\mathsf{rhsf}_2}^{(1)}$; $2\mathsf{rhsf}^{(1)} \rightleftarrows {\mathsf{rhsf}_2}^{(2)}$.

The refined model of [18] consists of 20 species and 55 irreversible reactions, compared to 10 species and 17 irreversible reactions in the basic model of [29]. The refined model is shown in Table 4 of the appendix.

4 Quantitative refinement in ODE models

The concept of quantitative model refinement of biomodels has been discussed and applied to an ODE model of the eukaryotic heat shock response in [18] . We recall it here briefly for the sake of completeness.

Consider the following notations:

$$\begin{aligned}
&\mathsf{Rhsf} = \mathsf{rhsf} + \mathsf{rhsf}^{(1)};\\
&\mathsf{Rhsf}_2 = \mathsf{rhsf}_2 + \mathsf{rhsf}_2{}^{(1)} + \mathsf{rhsf}_2{}^{(2)};\\
&\mathsf{Rhsf}_3 = \mathsf{rhsf}_3 + \mathsf{rhsf}_3{}^{(1)} + \mathsf{rhsf}_3{}^{(2)} + \mathsf{rhsf}_3{}^{(3)};\\
&\mathsf{Rhsf}_3\colon \mathsf{Rhse} = \mathsf{rhsf}_3\colon \mathsf{rhse} + \mathsf{rhsf}_3{}^{(1)}\colon \mathsf{rhse} + \mathsf{rhsf}_3{}^{(2)}\colon \mathsf{rhse}\\
&+\mathsf{rhsf}_3{}^{(3)}\colon \mathsf{rhse};\\
&\mathsf{Rhsp}\colon \mathsf{Rhsf} = \mathsf{rhsp}\colon \mathsf{rhsf} + \mathsf{rhsp}\colon \mathsf{rhsf}^{(1)}.
\end{aligned}$$

We recall next the lemma concerning the existence and uniqueness of solutions of systems of ODEs derived based on the principle of mass-action.

Lemma 1. *[16] Consider a molecular model and its associated system of ODEs derived based on the mass-action law. For any fixed initial condition, there exists an interval of the form* $[0, x), x \in \mathbb{R}_+ \cup \{+\infty\}$ *and a solution* ϕ *such that any other solution is a restriction of* ϕ*.*

The problem is how to set the kinetic parameters of the refined model so that the quantitative refinement conditions (2)-(4) are satisfied. An attempt to attain all solutions would require solving the non-linear systems of ODEs corresponding to the mass-action model for the basic and the refined heat shock response models, which cannot be done analytically. An alternative is to set the kinetic parameters of the refined model in such a way that the system of ODEs for variables Rhsf, Rhsf_2, Rhsf_3, $\mathsf{Rhsf}_3\colon \mathsf{Rhse}$, $\mathsf{Rhsp}\colon \mathsf{Rhsf}$, hsp, mfp, $\mathsf{hsp}\colon \mathsf{mfp}$, prot, hse is indistinguishable from the one corresponding to the basic heat shock response model, modulo a variable renaming; such a choice leads to the values in Table 5 of the appendix. The choice of initial values for the variables of the refined model imposes similar conditions for the initial and the refined model. Due to Lemma 1, the refinement conditions (2)-(4) are satisfied, thus the model in Table 4 of the appendix is a quantitative refinement of the initial model in Table 1.

The solution thus obtained is evidently not unique. For example, the kinetic rate constants of all reactions involving at least one form of acetylated hsf could be set to zero; such a choice would cancel the refinement since the influence of all acetylated variables would be ignored in the model. The approach in setting the values in Table 5 of the appendix was to consider all subspecies of a species

equally likely, without favouring any of them through the kinetics of the reactions they are involved in. The ODE models for the basic and the refined heat shock response models, and the ODEs corresponding to the sum of refined subspecies for each refined species are listed in Tables 6, 7, 8 of the appendix.

5 Quantitative refinement in Petri net models

We propose in this section a Petri net implementation of the heat shock response models, using Snoopy as the modeling tool, and Charlie for the analysis of the models. The refinement of the basic heat shock response model was implemented using colored Petri nets, with two approaches: one aimed to keep the same structure of the network (in terms of transitions), while the other focused on using as few colors as possible.

5.1 Petri nets and colored Petri nets

Petri nets are a sound formalism for representing systems with concurrency and resource sharing. For details on Petri nets, we refer to [31], [32], and consider in the following that the reader is familiar with basic concepts of Petri net theory. The main components of a Petri net are *places*, represented as circles, *transitions*, represented as squares, *arcs*, connecting a place with a transition or a transition with a place, and *tokens*, denoting the quantities available in each place. In a biological setup, the species of a biological system are represented as places, and the various reactions they take part in are represented as transitions.

Colored Petri nets are a framework extending Petri nets to allow a more compact representation of complex (e.g., biological) systems. Most often, complex systems have repeating patterns, or small variations of some species (mutations, post-transitional modifications) that are explicitly modeled. Instead, one might denote by a single colored place an entire class of such similar elements. The class has a *color set* with as many colors as the number of different elements in the class. Each element (subspecies) is then uniquely identified by its color,by means of colored tokens, and it is possible to define reactions that fire only for a subset of the class, using *guards* to select the desired transition instances. Color sets are in fact simple (int, enumeration) or compound types (cartesian product of two or more simple/compound types). For example, the dimerization of two different proteins can be represented as a single dimerization reaction with two colors, as depicted in Figure 1. The elements of a colored Petri net are similar to standard Petri net elements, with additional information encoding the colors. Tokens have colors, and places have a color set defining the possible colors for the tokens in that place. The flow of colored tokens in the network is defined through *arc expressions*, and the enabling of transitions can be subject to Boolean constraints (guards). For more details on colored Petri nets we refer to [19] and [25].

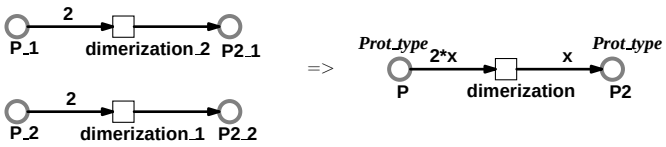

Figure 1: Representing the dimerization of two different proteins, P_1 and P_2 with a single colored Petri net, using a color set with two colors, *Prot_type* $= \{1, 2\}$. The choice between the two colors 1 and 2 is done by the variable x, i.e. when x=1, the reaction will consume two proteins with color 1 and produce one dimer with color 1, and when x=2, the reaction will consume two proteins with color 2 and produce one dimer with color 2. In the figure, all places and transitions have identifiers, and in the colored version we also list the corresponding color set (italic text) for each place.

5.2 The Snoopy and Charlie software tools

Snoopy [34] is a tool for designing and running Petri nets. It can run both deterministic and stochastic simulations. It supports basic Petri nets, as well as many extensions of Petri nets (out of which colored Petri nets are of particular interest in this report). In our implementation, we used the 02-05-2012 stable version of Snoopy under Windows.

In order to qualitatively analyze a network, Snoopy offers support for Charlie, a tool specially designed for analyzing Petri nets. Charlie can be used to check and compute several network properties. Two important properties for a Petri net are the places and transitions invariants (P- and T-invariants respectively). The P-invariants are sets of places with the property that their weighted sum of tokens is constant throughout the simulation, and thus they encode in a biochemical system the mass conservation relations. Moreover, any place belonging to a P-invariant is bounded. T-invariants are another important property of a network. They are integer vectors of transitions whose ordered firing can reproduce a start-point state, i.e. the total effect a T-invariant has on a place marking is null. In a biological setup, T-invariants can also be read as the relative firing rates of transitions at steady state. For more formal definitions of P- and T-invariants, see [14].

5.3 A Petri net for the basic HSR model

A standard Petri net model for the heat shock response was previously reported in [3]. We focus here on a Snoopy continuous Petri net implementation of the basic heat shock response model, shown in Figure 2. The network has 10 places and 17 transitions, encoding the 10 species and 17 irreversible reactions in the basic model definition of [29]. The numerical setup of our implementation is taken from the basic model definition. In order to compare the predictions of the model in [29] with our Snoopy implementation, we considered the DNA binding activity

of hsf's, for a simulation time of 14400 seconds. The DNA binding activity for 42°C (relative to the maximum value), together with the reported experimental values are presented in Figure 7.

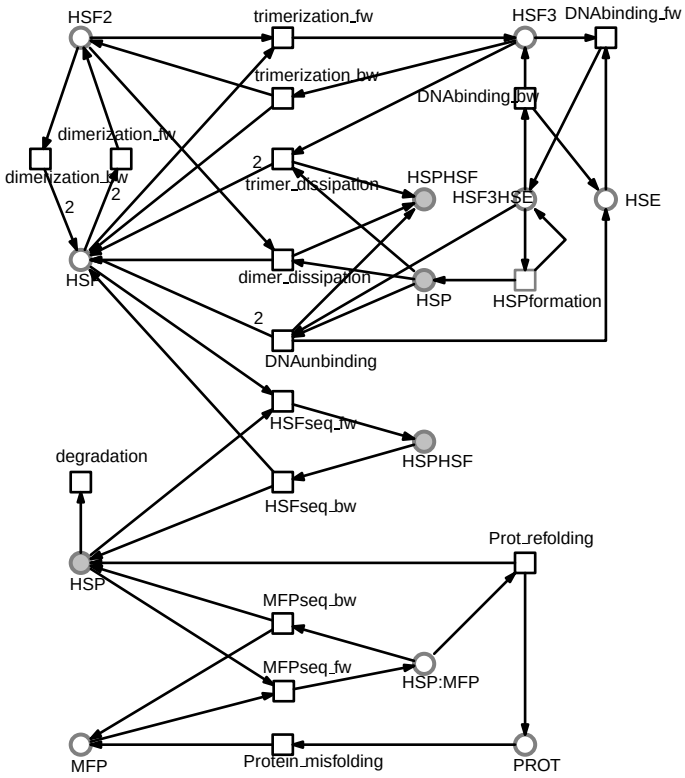

Figure 2: Snoopy implementation of the basic heat shock response model. The text next to a place (transition) denotes the identifier of that particular place (transition). Arc multiplicities greater than 1 are included in the picture. The dashed gray circles are logical places (they may appear several times, but they represent the same species).

Model validation required the analysis of several properties. For instance, the P-invariants reported by Charlie (and listed in Table 9 of the appendix) encode all the mass conservation relations reported in the ODE-based model of [29]. Moreover, all places except HSP are covered by P-invariants, which means they are bounded. The three mass conservation relations yield three constants (accounting for the total amount of HSF, HSE and protein molecules in the system, respectively), that have been used in the PRISM implementation of the model. The T-invariants for the basic model validate the model, in the sense that all successions of reactions whose firing overall effect on the system is null are present in a T-invariant. For example, the T-invariant containing the transitions dimerization_fw, trimerization_fw, HSFsequestration_bw, trimer_dissipation denotes a sequence of reactions that is needed in order to first produce (via first producing a dimer, then

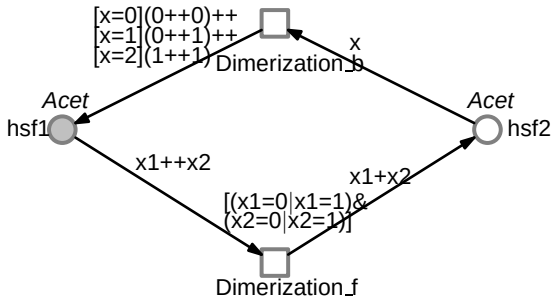

Figure 3: Modeling the hsf dimers using a color set with three colors, *Acet* $= \{0, 1, 2\}$. The identifiers of places and transitions are written in regular font, while the italic text next to places denotes the color set of the place. The monomers (hsf1) are represented using the same color set, to exemplify the use of guards in the forward transition, i.e. the condition that they can only have values 0 or 1. The preplaces of the forward reaction are two molecules of monomers, with colors x_1 and x_2. The result will be the production of one dimer with color (x_1+x_2). In the reverse reaction, one dimer with color x is split into two monomers according to its color (if x=0, it will produce two monomers with color 0, if x=1, it will produce one monomer with color 0 and one monomer with color 1, and if x=2, it will produce two monomers with color 1).

consuming that dimer to form a trimer, then dissipating it to produce a molecule of hsp: hsf) and then consume one token of hsp: hsf (via the HSFsequestration_bw reaction). The model is covered by T-invarians, as can be seen in Table 10 of the appendix containing the T-invariants as reported by Charlie.

5.4 Petri nets for the acetylation-refined HSR model

For the refined heat shock response that includes two types of hsf's (acetylated and non-acetylated [18]), we chose an implementation based on colored continuous Petri nets. There are several ways of reasoning about refined species within this framework. For example, the dimer of a protein with a site that can be acetylated (1) or non-acetylated (0) can be either seen as an entity with 0, 1, or 2 acetylated sites, or as a compound where the order of the acetylated sites counts (i.e. (0,0), (0,1), (1,0), (1,1)). Depending on the approach one takes, the colored representation will have different color sets, different number of transitions and different kinetic constants. We modeled the refined heat shock response using two approaches: one focused on keeping the structure of the basic model intact, with the same transitions and kinetic constants (we call this model *transition-focused*). This is the most compact representation. The other approach aimed to minimize the number of colors used in the model (we call this model *color-focused*).

During the modeling process, several choices had to be made. We detail here

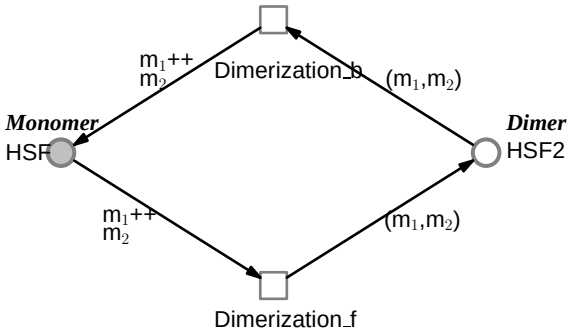

Figure 4: Modeling the hsf dimers using a compound color set *Dimer* = *Monomer* × *Monomer*. The regular text next to places and transitions denotes their respective identifier, while the color sets are written in italic font. The monomers (HSF) are represented using the color set *Monomer* $= \{0, 1\}$. The preplaces of the forward reaction are two molecules of monomers, with colors m_1 and m_2. The result will be the production of one dimer with color (m_1,m_2). In the reverse reaction, one dimer with color (m_1,m_2) is split into the two monomers m_1 and m_2 that it contains.

the modeling options for the dimerization and trimerization of acetylated and non-acetylated hsf's. There are three types of dimers that can be formed: non-acetylated dimer ($hsf_2{}^{(0)}$), single-acetylated dimer ($hsf_2{}^{(1)}$), and double-acetylated dimer($hsf_2{}^{(2)}$). One way of modeling the dimers is using a color set with three colors of type int (0, 1, and 2 denoting the number of acetylated sites), as in Figure 3. Another approach would be to consider the dimer as a cartesian product of hsf monomers (0 for non-acetylated, and 1 for acetylated). With this representation, there are four possible dimers: (0,0), (0,1), (1,0) and (1,1). Although the mono-acetylated dimers (0,1) and (1,0) are biologically the same, they are modeled as different species, see Figure 4. The second approach offers a more compact representation, but the tradeoff is introducing an extra color in the model and thus extra transition instantiations for all reactions that place can be part of.

When modeling hsf trimers, one could consider for example three color sets: a color set $\mathsf{Tri} = \{0, 1, 2, 3\}$, a compound color set $\mathsf{Compound} = \{0, 1\} \times \{0, 1, 2\}$, or a compound set $\mathsf{Trimer} = \{0, 1\} \times \{0, 1\} \times \{0, 1\}$. The first approach uses as few colors as possible, at the cost of a complicated representation, with many conditions in a transition, and also introducing new transitions in the colored representation (see Figure 9 of the appendix). The last approach (transition-focused) is the most compact, the tradeoff being an increased number of colors. The second approach is a combination of the other two: it uses 6 colors, and additional transitions are required.

The transition-focused refined model is presented in Figure 8 of the appendix. The initial concentrations, as well as the rate constants are set as in the ODE model of [18]. The number of places and transitions is the same as in the basic

model. The entire complexity is encapsulated in the colors of the places and the arc expressions (which select several possible combinations of places). For a complete description of the models in terms of arc expressions, guards, kinetics and initial concentrations, check the Snoopy models available online at `http://goo.gl/eTTA7h`.

When simulating a colored Petri net, Snoopy first unfolds it, in other words it creates an equivalent Petri net. Each place instance (each color) will correspond to a place in the unfolded net, and each transition instance (each binding) will correspond to a transition in the unfolded net; for details on colored Petri nets unfolding, see [26]. The unfolded network contains 29 places and 77 transitions, as opposed to 10 places and 17 transitions for the colored model. The tremendous advantage of colored Petri nets lies in the compact representation of complex [biological] systems.

The color-focused refined model is presented in Figure 9 of the appendix. As shown in the figure, all reactions involving the decomposition of complexes containing hsf's required additional transitions. For example, the trimer dissipation reaction $\mathsf{hsf}_3 + \mathsf{hsp} \rightarrow \mathsf{hsp{:}\,hsf} + 2\,\mathsf{hsf}$ is split into three transitions. One covers the case when all hsf's in the trimer have the same acetylation value (i.e. hsf_3 has color 0 or 3). In this case, there is no distinction between which hsf binds to hsp and which two hsf's become unbound, and the kinetic constant for this transition is the same as the corresponding one in the basic model. When hsf_3 has color 1 or 2, there are two binding possibilities: either hsp binds to a non-acetylated hsf (freeing one non-acetylated hsf and one acetylated hsf if hsf_3 has color 1, or two acetylated hsf's if hsf_3 has color 2), or hsp binds to an acetylated hsf (freeing two non-acetylated hsf's if hsf_3 has color 1, or one non-acetylated hsf and one acetylated hsf if hsf_3 has color 2). For the two transitions representing these possibilities, the kinetic constant is half of the corresponding one in the basic model (following the reasoning explained in [18]). This model has 10 places and 25 transitions, and its corresponding flattened Petri net has 20 places and 56 transitions. It follows that this representation, although more complex than the transition-focused one, encodes a smaller network, reducing thus the simulation run time. The DNA binding activity predicted by the two models is depicted in Figure 7. Both the transition- and color-based refinements have been compared with the basic model predictions, and they are all equivalent (data not shown).

6 Quantitative refinement in rule-based models

6.1 Basic concepts

Within a rule-based modelling framework, a model is specified primarily by determining the molecules of interest, their components (i.e. a post-translational modification site) and the states corresponding to each component. A molecule

can be graphically represented by a unit-box, comprising the components of each molecule as nodes, see Figure 5. Molecular interactions are consequently represented as graph-rewriting rules. A rule corresponds to a certain type of reaction or to a class of reactions, depending on its specificity, see [9].

The binding between two molecules can be indicated graphically, for instance, by adding edges between the nodes in the unit-boxes. The unbinding is characterized by the removal of an edge connecting two nodes. A post-translational modification of a protein at some specific site is indicated by the change in the state of a specific site of the protein. A rule specifies "group rules", which define molecules or complexes of molecules with certain common syntactic attributes, partially describing the interaction of the components and/or states of the molecules, see [9, 10]. A rule is characterized by two group rules, corresponding to the set of reactants and the set of reactions, respectively. This correspondence is graphically emphasized by an arrow directed from reactants to products, see Figure 5. A kinetic law is to be associated with every rule, see [10]. All reactions encoded by a particular rule follow the same rate law. However, distinct reactions may be specified through different rate constants, some of which require the multiplication by diverse factors, generated by collision frequency among identical molecules, numerous analogous paths from the substrates to the products of a reaction, symmetry of the patterns that the generating rule was applied on, etc. We refer the re

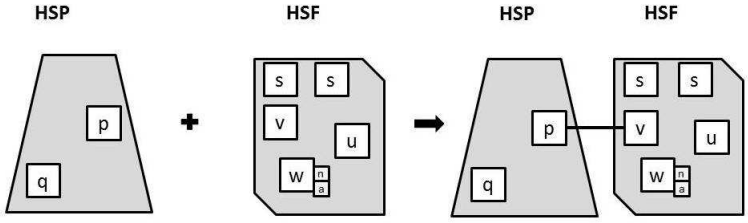

Figure 5: A graphical representation of the species HSP (containing sites 'p' and 'q') and HSF (containing sites 's','u','v','w') and of the rule showing the sequestration of HSFs, illustrated by binding the 'p' site of HSP with the 'v' site of HSF. Note the two possible states of the site 'w', namely 'a' and 'n', which depict two possible states of the species, acetylated or non-acetylated respectively.

6.2 Bionetgen and RuleBender

Bionetgen is a description language and a rule-based framework designed for the construction and analysis of large computational biomodels, depicting, for instance, signal transduction systems, which take into consideration diverse interactions of molecular domains, such as post-translational modifications, etc, see [5]. A Bionetgen input file consists of a series of definitions for the molecular species and their components, reaction rules, kinetic rate constants, initial concentrations

and simulation commands. The simulation can be done either deterministically using ODEs or stochastically, using SSA algorithms, see [36, 39].

A model is specified in Bionetgen by defining its molecules, their binding sites and the states for specific domains, corresponding for instance to some post-translational modifications, such as aceytlation, phosphorylation, ubiquitation, etc. A rule is characterized by the set of reactants, the set of products and the kinetic law that governs the dynamics for the reaction or the class of reactions that the rule represents, [36]. Taking the example of hsf sequestration in Figure 5, one can write the corresponding rule in Bionetgen as follows: $\mathsf{HSP}(p,q) + \mathsf{HSF}(s,s,u,v) \leftrightarrow \mathsf{HSP}(p!1,q).\mathsf{HSF}(s,s,u,v!1)$. Note that a bound is specified by adding an index preceded by an exclamation mark to the binding site. Bionetgen generates a reaction network that may then be used to simulate the dynamics of the system deterministically or stochastically, see [36].

RuleBender is an open source visualizer for rule-based modelling that allows compiling large models, being very suitable for debugging, simulation and analysis of rule-based models. The simulation is performed through a Bionetgen simulator, [39]. The simulation generates a reaction network, represented both in SBML and NET format, and graphs for each species in the model, and for diverse group rules, [36].

6.3 A RuleBender implementation of the basic HSR model

This section focuses on the RuleBender implementation of the basic heat shock response model, as introduced in Section 2. We model all reactions to follow the principle of mass action. Conforming to the implementation presented here, Bionetgen source code comprises a set of twelve rules, which generate a total number of seventeen irreversible reactions. The kinetic rate constants and the initial values for the reactants were set conforming to [29]. Due to the symmetry that some of the species exhibit, the collision frequency (e.g. in our case dimerization, trimerization, etc) and the existence of multiple paths from substrates to products in some reactions (e.g. for the heat shock response model, the unbinding of trimers), kinetic rate constants for those specific reactions are multiplied in Bionetgen by diverse symmetry and/or statistical factors, see [4]. For example, the collision frequency of two different types of reactants A and B, $A+B$, is twice that of identical types of reactants $A + A$. Another example concerns the multiple reaction paths from reactants to products, which may generate statistical factors. Preserving the fit of the heat shock response model attained in [29] required a multiplication of some rate constants by the inverse of the aforementioned factors respectively.

RuleBender generates during the process of model development a contact map which depicts the connectivity between the molecules. The contact map for the basic model of the heat shock response is shown in Figure 6.

One can notice in Figure 6 that hsf's have been represented as having 4 sites

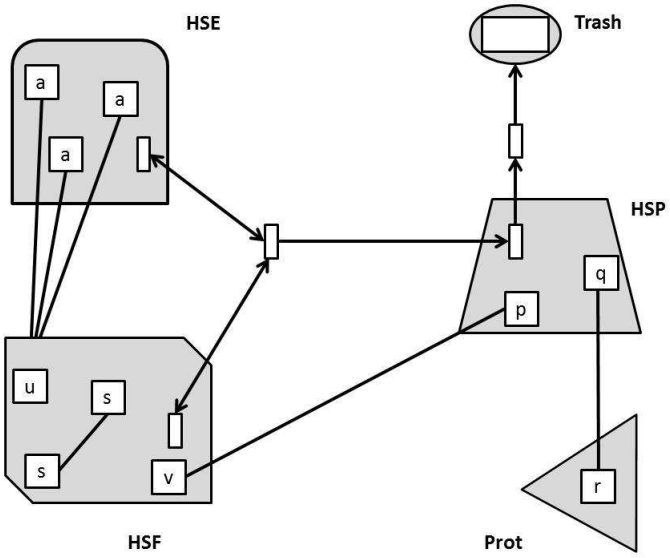

Figure 6: The RuleBender generated contact map for the basic model of the heat shock response. It depicts the possible interconnections among the model's species.

(s, s, u, v). The two s sites are involved in the generation of dimers and trimers. The other two sites, u and v, are used to illustrate the process of DNA binding/unbinding and hsf sequestratation/dimer (trimer) dissipation. Trimers are considered to be circular structures, each of the 's' site of one hsf being bound to the 's' sites of the consequent hsf's, no two hsf's having both sites 's' bound to the same partner. The promoter, hse, has been represented as having three identical sites (a, a, a), so as to be connected to the trimer in such a way that the symmetry is not affected. Heat shock proteins are modeled to have two sites 'p' and 'q', used for the modelling of unbinding of dimers and trimers and for the sequestration of misfolded proteins. The model takes into account a species called Prot, which has a site with two possible states, one of which accounts for misfolded proteins 'm' and another one 'f', that accounts for folded proteins. A "dummy" component, called *Trash*, has been introduced to help encode the degradation of heat shock proteins.

The contact map in Figure 6 illustrates the connectivity between the species in the model. The link between the 's' sites of the hsf molecule denotes the formation of dimers and trimers through the agency of these sites. Once trimers are formed, they can bind to the heat shock element (hse), the connection being illustrated by three links connecting hsf trimers to the heat shock element (one can notice three 'a' sites the heat shock element component exhibits). The middle connector encodes for a number of reactions, such as: DNA unbinding, HSP synthesis and breaking of dimers and trimers. The link between the site 'v' of the hsf component and the site 'p' of the hsp component illustrates hsf sequestration. The link between the hsp component and the prot component encodes the following

reactions: protein misfolding, protein refolding and mfp sequestration. By linking the component $Trash$ to the hsp component, we encoded for the degradation of hsp's.

We chose a deterministic simulation for the basic model. The simulation results for DNA binding for a temperature of 42°C are shown in Figure 7. The plot shows that RuleBender prediction is in accordance with the results reported in [29].

6.4 A RuleBender implementation of the acetylation-refined HSR model

We focus in this section on the acetylation-refinement of the heat shock response, as described in [18]. There are several changes to do in Rulebender to refine the basic model so as to include the acetylation of hsf's. The syntax of the rules remains, in this case, unchanged, since all reactions, in this model, take place regardless of the acetylation status of the molecules. We brought changes in the definition of hsf's, by introducing one acetylation site, 'w', which can be either acetylated or not, and in the initial concentrations of the molecules. The initial concentrations were set conforming to [18].

The simulation of the refined model for a temperature of 42°C is shown in Figure 7. The graph shows that the Rulebender prediction for the refined model and the one for the basic model are indistinguishable.

7 Quantitative refinement in PRISM models

PRISM is a free and open source guarded command language and probabilistic model checker [22]. It can be used to model and analyze a wide range of probabilistic systems including communication and multimedia protocols, randomized distributed algorithms, security protocols, biological systems, etc. PRISM supports several types of probabilistic models: probabilistic automata (PAs), probabilistic timed automata (PTAs), discrete-time Markov chains (DTMCs), continuous-time Markov chains (CTMCs), Markov decision processes (MDPs), see [22]. A PRISM model consists of a keyword which describes the model type (e.g. CTMC) and a set of modules whose states are defined by the state of their finite range variables (e.g., $\mathsf{hsf}, \mathsf{hsf}_2, \mathsf{hsf}_3$, etc.). The state of the variables in each module is specified by some commands including a guard and one or more updates [22].

7.1 A PRISM implementation of the basic HSR model

We implemented the basic heat shock response as a CTMC model that defines all possible guards (in this case reactions) within a single module. The PRISM

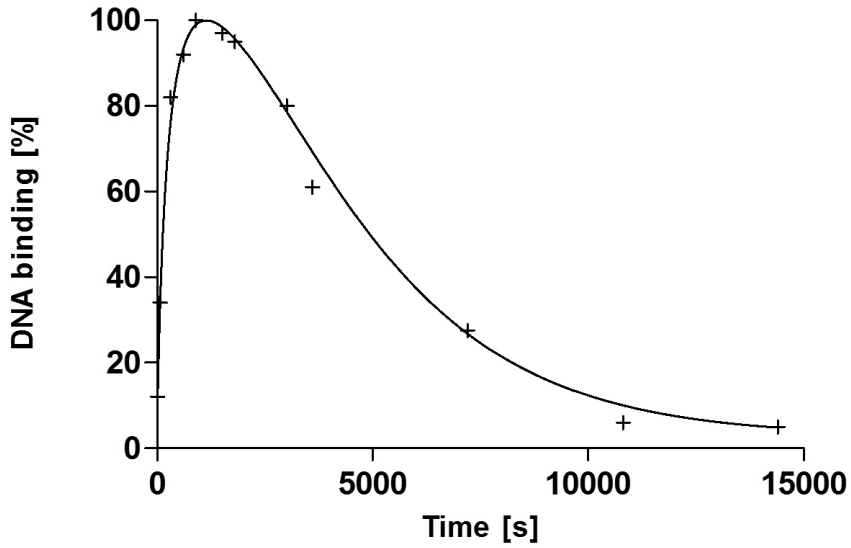

Figure 7: DNA binding for the heat shock response, as predicted by the ODE-based, the Petri net-based and the rule-based models. The graph shows that all these models confirm the experimental data of [21], for a temperature of 42°C. The curve represents the predictions of the models for the total amount of hse-bounded hsf trimers (both in the case of the basic model and the refined model), correlated with the experimental data shown as crossed points; both are relative to their maximum values.

model consists of 10 variables, each of them corresponding to one of the reactants in the model, and 17 guards representing the 17 irreversible reactions of the system. The values for upper bounds of the variables are taken from our Petri net model's p-invariants and mass-conservation relations. Upper bounds are used both for allocating memory and in the guarded commands. For example the guard corresponding to *dna binding* is expressed as follows:

[dnabinding]
$\mathsf{hsf}_3 >= 1 \wedge \mathsf{hse} >= 1 \wedge \mathsf{hsf}_3\colon \mathsf{hse} <= N-1 \rightarrow$
$\mathsf{hsf}_3 * \mathsf{hse} * k_5 : (\mathsf{hsf}_3{}' = \mathsf{hsf}_3 - 1) \wedge (\mathsf{hse}' = \mathsf{hse} - 1) \wedge$
$\wedge (\mathsf{hsf}_3\colon \mathsf{hse}' = \mathsf{hsf}_3\colon \mathsf{hse} + 1)$,
where N represents the upper bound for hse in the system.

The PRISM model can be found at `http://goo.gl/ULYkuU`, and is listed in Table 11 of the appendix. It is noteworthy to mention that the PRISM model could be obtained from the Petri net model via some format manipulations in Snoopy. However, we decided to write the model from scratch in order to be able to compare the modeling effort in each chosen framework.

7.2 A PRISM implementation of the acetylation-refined HSR model

The approach we took in Sections 5 and 6 to implement the acetylation-refined heat shock response model was through a compact representation of the acetylated species. Whereas colors of the places and arc expressions were employed to represent the refinement in the Petri net model, in modeling with RuleBender the solution was to introduce a new acetylation site for every hsf molecule. Both methods used structured data types for the species, thus concealing the complexity of the model in a compact representation. In PRISM this requires a method to represent the acetylation details in the definition of hsf, i.e. a composite data type. Since PRISM currently supports only simple data type (e.g. integer, boolean) variables in the model, such a definition is not possible. Alternatively, we implemented the acetylation-refined model through introducing new variables describing all possible acetylation configurations of hsf and hsf complexes. This was similar to the ODE-based approach to quantitative model refinement discussed in [18].

The refined heat shock response model is built based on the refinements given in Section 3.2 by refining all reactants and complexes involving hsf. In this approach, the strategy is to replace each guard involving any refined reactant by the guards considering all possible refined reactions. For example for *dna binding*, the following guards are considered in the refined PRISM model:

$$
\begin{aligned}
&\textbf{[]}\ \mathsf{rhsf_3} >= 1 \wedge \mathsf{rhse} >= 1 \wedge \mathsf{rhsf_3{:}\,rhse} <= N-1 \rightarrow \\
&\mathsf{rhsf_3} * \mathsf{rhse} * k_5 : (\mathsf{rhsf_3}' = \mathsf{rhsf_3} - 1) \\
&\wedge (\mathsf{rhse}' = \mathsf{rhse} - 1) \wedge (\mathsf{rhsf_3{:}\,rhse}' = \mathsf{rhsf_3{:}\,rhse} + 1);
\end{aligned}
$$

$$
\begin{aligned}
&\textbf{[]}\ \mathsf{rhsf_3}^{(1)} >= 1 \wedge \mathsf{rhse} >= 1 \wedge \mathsf{rhsf_3{:}\,rhse}^{(1)} <= N-1 \rightarrow \\
&\mathsf{rhsf_3}^{(1)} * \mathsf{rhse} * k_5 : (\mathsf{rhsf_3}^{(1)'} = \mathsf{rhsf_3}^{(1)} - 1) \\
&\wedge (\mathsf{rhse}' = \mathsf{rhse} - 1) \wedge (\mathsf{rhsf_3{:}\,rhse}^{(1)'} = \mathsf{rhsf_3{:}\,rhse}^{(1)} + 1);
\end{aligned}
$$

$$
\begin{aligned}
&\textbf{[]}\ \mathsf{rhsf_3}^{(2)} >= 1 \wedge \mathsf{rhse} >= 1 \wedge \mathsf{rhsf_3{:}\,rhse}^{(2)} <= N-1 \rightarrow \\
&\mathsf{rhsf_3}^{(2)} * \mathsf{rhse} * k_5 : (\mathsf{rhsf_3}^{(2)'} = \mathsf{rhsf_3}^{(2)} - 1) \\
&\wedge (\mathsf{rhse}' = \mathsf{rhse} - 1) \wedge (\mathsf{rhsf_3{:}\,rhse}^{(2)'} = \mathsf{rhsf_3{:}\,rhse}^{(2)} + 1);
\end{aligned}
$$

$$
\begin{aligned}
&\textbf{[]}\ \mathsf{rhsf_3}^{(3)} >= 1 \wedge \mathsf{rhse} >= 1 \wedge \mathsf{rhsf_3{:}\,rhse}^{(3)} <= N-1 \rightarrow \\
&\mathsf{rhsf_3}^{(3)} * \mathsf{rhse} * k_5 : (\mathsf{rhsf_3}^{(3)'} = \mathsf{rhsf_3}^{(3)} - 1) \\
&\wedge (\mathsf{rhse}' = \mathsf{rhse} - 1) \wedge (\mathsf{rhsf_3{:}\,rhse}^{(3)'} = \mathsf{rhsf_3{:}\,rhse}^{(3)} + 1);
\end{aligned}
$$

One could also use parallel modules to implement the refinement but this approach would not help reducing the complexity of the model.

The complete PRISM implementation of the refinement is listed in Table 12 of the appendix. The numerical setup of this model is based on [18].

7.3 Model checking of the HSR models

According to [23], the maximum number of states that PRISM can handle for CTMCs is 10^{10}. In both our models (basic and refined version of the heat shock response), the number of all possible states in the system exceeds this limit. This is a known problem for biological systems in PRISM, see [13]. Several studies have addressed this issue, see e.g. [24, 15, 22, 13]. One of the investigated approaches is *approximate verification* of probabilistic systems, where a Monte-Carlo algorithm is used to approximate the probability of a temporal formula to be true, see [24, 15]. We used this method to verify the desired properties of the heat shock response model. In this approach a large number of stochastic paths is sampled for the model and based on the defined properties, the result for each run is obtained. The information produced in this way gives an approximate result for the probability that the desired property holds for the model.

We are interested in verifying two properties discussed in [29]. The properties are: (i) the validity of three mass-conservation relations and (ii) the level of DNA binding eventually returns to the basal values, both at $37°C$ and at $42°C$.

In order to check the mass conservation properties, we used the G operator which checks if the property remains true at all states along the path. The three properties we were interested in are listed as follows:

- $p =?$ [G $\mathsf{hsf} + 2\,\mathsf{hsf}_2 + 3\,\mathsf{hsf}_3 + 3\,\mathsf{hsf}_3{:}\,\mathsf{hse} + \mathsf{hsp}{:}\,\mathsf{hsf} = \mathsf{hsf}_{const}$],
- $p =?$ [G $\mathsf{hse} + \mathsf{hsf}_3{:}\,\mathsf{hse} = \mathsf{hse}_{const}$],
- $p =?$ [G $\mathsf{prot} + \mathsf{mfp} + \mathsf{hsp}{:}\,\mathsf{mfp} = \mathsf{prot}_{const}$],

where $\mathsf{hsf}_{const}, \mathsf{hse}_{const}$ and prot_{const} represent the total amounts of $\mathsf{hsf}, \mathsf{hse}$ and prot respectively. These properties check if the mass-conservation relations, corresponding to the level of $\mathsf{hsf}, \mathsf{hse}$ and prot, are valid in all the states. In each case, the value of p was confirmed to be one, which was to be expected, with confidence level 95%, i.e. the mass conservation laws are respected in the model.

For the second property, we verified in PRISM that for time points larger than 14400, the value of $\mathsf{hsf}_3{:}\,\mathsf{hse}$ reactants returns to their initial value. We formulated the following property:

$$p =? \quad [F >= 14400 \quad \mathsf{hsf}_3{:}\,\mathsf{hse} = 3].$$

The probability value calculated by PRISM was one for this property as well, with confidence level 95%.

We also checked if the model confirms the experimental data of [21] on DNA binding. One approach could be to run the simulation for many times and plot the average run. Due to the memory issues of the PRISM, we were not able to follow this approach. Since we are using a stochastic model, our second approach was to check the probability of having a data point within the interval $[0.9 \cdot d, 1.1 \cdot d]$ in

Table 2: Model checking of basic heat shock response model with PRISM for the total level of $\mathsf{hsf_3}$: hse

Property	Probability
$p =?\ [F[40, 80]\ 8 <= \mathsf{hsf_3}\text{: hse} \,\&\, \mathsf{hsf_3}\text{: hse} <= 10]$	0.90
$p =?\ [F[270, 330]\ 20 <= \mathsf{hsf_3}\text{: hse} \,\&\, \mathsf{hsf_3}\text{: hse} <= 25]$	0.86
$p =?\ [F[540, 660]\ 22 <= \mathsf{hsf_3}\text{: hse} \,\&\, \mathsf{hsf_3}\text{: hse} <= 28]$	0.80
$p =?\ [F[810, 990]\ 24 <= \mathsf{hsf_3}\text{: hse} \,\&\, \mathsf{hsf_3}\text{: hse} <= 30]$	0.93
$p =?\ [F[1350, 1650]\ 24 <= \mathsf{hsf_3}\text{: hse} \,\&\, \mathsf{hsf_3}\text{: hse} <= 30]$	0.85
$p =?\ [F[1620, 1980]\ 23 <= \mathsf{hsf_3}\text{: hse} \,\&\, \mathsf{hsf_3}\text{: hse} <= 29]$	0.84
$p =?\ [F[2700, 3300]\ 20 <= \mathsf{hsf_3}\text{: hse} \,\&\, \mathsf{hsf_3}\text{: hse} <= 24]$	0.91
$p =?\ [F[3240, 3960]\ 15 <= \mathsf{hsf_3}\text{: hse} \,\&\, \mathsf{hsf_3}\text{: hse} <= 19]$	0.90
$p =?\ [F[6480, 7920]\ 6 <= \mathsf{hsf_3}\text{: hse} \,\&\, \mathsf{hsf_3}\text{: hse} <= 9]$	0.82
$p =?\ [F[9720, 11880]\ 1 <= \mathsf{hsf_3}\text{: hse} \,\&\, \mathsf{hsf_3}\text{: hse} <= 2]$	0.65
$p =?\ [F[12960, 15840]\ 1 <= \mathsf{hsf_3}\text{: hse} \,\&\, \mathsf{hsf_3}\text{: hse} <= 2]$	0.89

the time period $[0.9 \cdot t, 1.1 \cdot t]$, where d is the experimental data point at time t. The properties and their corresponding probabilities for the basic and refined models are given in Tables 2 and 3, respectively. The confidence interval for all the properties and the number of simulations were 95% and 150 respectively. We interpret the high values we obtained as a result as a confirmation that the two PRISM models are in accordance with the experimental data of [21].

8 Discussion

We focused in this paper on analyzing the capability of four different frameworks to implement the concept of quantitative model refinement: ODEs, Petri nets (with Snoopy), rule based modelling (with Bionetgen) and guarded command languages (with PRISM). Handling the combinatorial explosion due to accounting for a post-translational modification throughout our refinement proved to be fundamentally

Table 3: Model checking of refined heat shock response model with PRISM for the total level of $\mathsf{rhsf_3{:}\,rhse}$, where $T_{\mathsf{hsf_3{:}hse}} = \sum_{i=1}^{3} \mathsf{rhsf_3{:}\,rhse}^i$

Property	Probability
$p =? \, [F[40, 80] \; 8 <= T_{\mathsf{hsf_3{:}hse}} \& T_{\mathsf{hsf_3{:}hse}} <= 10]$	0.86
$p =? \, [F[270, 330] \; 20 <= T_{\mathsf{hsf_3{:}hse}} \& T_{\mathsf{hsf_3{:}hse}} <= 25]$	0.81
$p =? \, [F[540, 660] \; 22 <= T_{\mathsf{hsf_3{:}hse}} \& T_{\mathsf{hsf_3{:}hse}} <= 28]$	0.81
$p =? \, [F[810, 990] \; 24 <= T_{\mathsf{hsf_3{:}hse}} \& T_{\mathsf{hsf_3{:}hse}} <= 30]$	0.95
$p =? \, [F[1350, 1650] \; 24 <= T_{\mathsf{hsf_3{:}hse}} \& T_{\mathsf{hsf_3{:}hse}} <= 30]$	0.76
$p =? \, [F[1620, 1980] \; 23 <= T_{\mathsf{hsf_3{:}hse}} \& T_{\mathsf{hsf_3{:}hse}} <= 29]$	0.83
$p =? \, [F[2700, 3300] \; 20 <= T_{\mathsf{hsf_3{:}hse}} \& T_{\mathsf{hsf_3{:}hse}} <= 24]$	0.89
$p =? \, [F[3240, 3960] \; 15 <= T_{\mathsf{hsf_3{:}hse}} \& T_{\mathsf{hsf_3{:}hse}} <= 19]$	0.73
$p =? \, [F[6480, 7920] \; 6 <= T_{\mathsf{hsf_3{:}hse}} \& T_{\mathsf{hsf_3{:}hse}} <= 9]$	0.78
$p =? \, [F[9720, 11880] \; 1 <= T_{\mathsf{hsf_3{:}hse}} \& T_{\mathsf{hsf_3{:}hse}} <= 2]$	0.61
$p =? \, [F[12960, 15840] \; 1 <= T_{\mathsf{hsf_3{:}hse}} \& T_{\mathsf{hsf_3{:}hse}} <= 2]$	0.91

different in the approaches we considered. These modeling methods are not restricted to the analysis of our case study solely, but their applicability extends to other reaction-based models. Rule-based modelling tackles the complexity of refinement through a compact model representation based on a partial presentation of the details of the model species, leading to more effective model construction and analysis techniques. Colored Petri nets integrate programmability by including data types (color sets) as an intrinsic property of places. The color set assignation reflects on the structure of the network, affecting the dimensions of the corresponding flattened network. PRISM model checker promotes a low level implementation of data structures and, does not allow the modeler to introduce more complex data structures.

The rule based modelling approach to quantitative model refinement required the addition of a new domain to the hsf molecule type and bringing a change in the kinetic rate constants for some reactions. Symmetric rules in particular need to be considered carefully. Whereas the *rate law* is identical for all reactions en-

coded by a rule, some *rate constants* corresponding to particular reactions need to be altered, see [9]. Given a particular reaction from a family of reactions generated by a rule, its kinetic rate constant might require a multiplication by diverse factors so as to remain coherent with the other reactions generated by the same rule. Collision frequency factors emerge, for instance, when a reactions involves identical reactants. The collision frequency of a reaction of the form $A + A \to C$ is half of the collision frequency of a reaction of the form $A + B \to C$. Statistical factors may emerge also due to symmetry, either due to the existence of manifold analogous reaction paths from substrates to products, or to reaction rules altering patterns symmetry, see [9, 4]. To account for this, the Bionetgen implementation required a change in the kinetic rate constants for the forward reactions corresponding to dimerization, trimerization, DNA binding, DNA unbinding, trimer dissipation.

Refining a model in the basic Petri nets framework requires explicitly representing all new subspecies and manually refining all reactions they take part in. This combinatorial explosion of a model's size can be tackled by a careful manipulation of colors. There are several possible coloring schemes for the same model, and the modeling choice resumes to a tradeoff between the number of colors (directly affecting the number of places, and hence the number of transitions generated in the flattened Petri net) and the number of transitions in the colored model. It is possible to preserve the same structure of the network, by using compound color sets for all compound species, but this results in a large amount of colors, and this translates into an even larger flattened network. For complex biological models, this kind of approach on refinement might become infeasible due to computational limitations. Another method of refining a colored Petri net model is to focus on minimizing the number of colors. This method might require an additional step of adding conditional transitions for some reactions (e.g. trimer dissipation), but the corresponding flattened Petri net is smaller, and thus simulations run faster.

Unlike the two other approaches, we were not able to conceal the complexity of the refined model by defining variables including some internal information, due to the fact that the choice of variables type in PRISM is limited to simple data types. Therefore, the PRISM implementation of the refined model required an explicit description, similar to the data refinement in [18]. Model verification was based on approximate model checking, which resulted in a successful verification of several properties of the model, including three mass conservation relations. We could also verify that the data produced by the model agrees with the experimental data of [21] with high probability.

Our study shows that some modeling frameworks are more suitable for model refinement than others, with respect to the compactness of the representation of the refined model. A key ingredient for this is the spectrum of internal data structures supported by the modeling software. Data structures may encapsulate a large amount of information, and their effective manipulation can substantially reduce

the complexity of a model's representation. RuleBender provides data structures suitable for modeling biological systems: species, sites, links, partial description of species, rendering a straightforward refinement procedure with a very compact representation. In contrast, Petri nets are not primarily a biology-focused framework. Colored Petri nets introduce programmability in this modeling formalism, incorporating data types into the places of the network. New data types can be implemented based on primitive built-in types and composition rules. In refining a Petri net model, one has to define the appropriate data structures, and associate a biological meaning to each of them. The modeling choices affect both the compactness of the representation and the complexity of the corresponding expanded Petri net model. PRISM on the other hand only supports primitive data types. This translates into an explicit detailing of all elements of the refined model.

Our study shows that quantitative model refinement is a potentially viable approach to building a large biomodel. The approach can be used together with a multitude of modeling paradigms, allowing the modeler to increase the level of details of the model, while preserving its numerical behavior. Moreover, on any level of detail one can switch from a modeling paradigm to another, taking full advantage of the various analysis tools made possible in different model formulations, in terms of fast simulations, model checking or compact model representation. While our case-study shows the potential of the quantitative model refinement approach to model building, its scalability remains to be tested on a larger case study.

Acknowledgements

The authors thank Monika Heiner for her help with issues related to Snoopy and Charlie, James Faeder and Leonard Harris for advice on the Bionetgen implementation of the heat shock response, and Adam Smith for technical support regarding RuleBender.

References

[1] T. Arnesen. Towards a functional understanding of protein n-terminal acetylation. *PLoS Biology*, 9(5), 2011.

[2] L. Arthur. The edges of understanding. *BMC Biology*, 8:40, 2010.

[3] R.J. Back, T.O. Ishdorj, and I. Petre. A petri-net formalization of heat shock response model. In *Proceedings of COMPMOD 2008*, pages 53–61, 2008.

[4] M. Blinov, J. Yang, J. Faeder, and W. Hlavacek. Graph theory for rule-based modeling of biochemical networks. *Transactions on Computational Systems Biology VII*, pages 89–106, 2006.

[5] M.L. Blinov, J.R. Faeder, B. Goldstein, and W.S. Hlavacek. Bionetgen: software for rule-based modeling of signal transduction based on the interactions of molecular domains. *Bioinformatics*, 20(17):3289–3291, 2004.

[6] C. Choudhary, C. Kumar, F. Gnad, M.L. Nielsen, M. Rehman, T.C. Walther, J.V. Olsen, and M. Mann. Lysine acetylation targets protein complexes and co-regulates major cellular functions. *Science*, 325(5942):834–840, 2009.

[7] E. Czeizler, V. Rogojin, and I. Petre. The phosphorylation of the heat shock factor as a modulator for the heat shock response. In *Proceedings of the 9th International Conference on Computational Methods in Systems Biology*, pages 9–23. ACM, 2011.

[8] V. Danos, J. Feret, W. Fontana, R. Harmer, and J. Krivine. Rule-based modelling and model perturbation. *Transactions on Computational Systems Biology XI*, pages 116–137, 2009.

[9] J.R. Faeder, M.L. Blinov, B. Goldstein, and W.S. Hlavacek. Rule-based modeling of biochemical networks. *Complexity*, 10(4):22–41, 2005.

[10] J.R. Faeder, M.L. Blinov, and W.S. Hlavacek. Graphical rule-based representation of signal-transduction networks. In *Proceedings of the 2005 ACM symposium on Applied computing*, pages 133–140. ACM, 2005.

[11] M.A. Glozak, N. Sengupta, X. Zhang, and E. Seto. Acetylation and deacetylation of non-histone proteins. *Gene*, 363:15–23, 2005.

[12] Russ Harmer. Rule-based modelling and tunable resolution. *EPTCS*, 9:65–72, 2009.

[13] J. Heath, M. Kwiatkowska, G. Norman, D. Parker, and O. Tymchyshyn. Probabilistic model checking of complex biological pathways. In *Computational Methods in Systems Biology*, pages 32–47. Springer, 2006.

[14] Monika Heiner, David Gilbert, and Robin Donaldson. Petri nets for systems and synthetic biology. In *Formal methods for computational systems biology*, pages 215–264. Springer, 2008.

[15] A. Hinton, M. Kwiatkowska, G. Norman, and D. Parker. Prism: A tool for automatic verification of probabilistic systems. *Tools and Algorithms for the Construction and Analysis of Systems*, pages 441–444, 2006.

[16] M.W. Hirsch, S. Smale, and R.L. Devaney. *Differential equations, dynamical systems, and an introduction to chaos*. Academic Press, 2012.

[17] CS Hwang, A. Shemorry, A. Varshavsky, et al. N-terminal acetylation of cellular proteins creates specific degradation signals. *Science*, 327(5968):973–977, 2010.

[18] B. Iancu, El. Czeizler, Eu. Czeizler, and I. Petre. Quantitative refinement of reaction models. *International Journal of Unconventional Computing*, In Press, 2013.

[19] K. Jensen. Coloured petri nets: A high level language for system design and analysis. *Advances in Petri nets 1990*, pages 342–416, 1991.

[20] H. Kitano. Systems biology: a brief overview. *Science*, 295(5560):1662–1664, 2002.

[21] M.P. Kline and R.I. Morimoto. Repression of the heat shock factor 1 transcriptional activation domain is modulated by constitutive phosphorylation. *Molecular and cellular biology*, 17(4):2107–2115, 1997.

[22] M. Kwiatkowska, G. Norman, and D. Parker. PRISM 4.0: Verification of probabilistic real-time systems. In G. Gopalakrishnan and S. Qadeer, editors, *Proc. 23rd International Conference on Computer Aided Verification (CAV'11)*, volume 6806 of *LNCS*, pages 585–591. Springer, 2011.

[23] Marta Kwiatkowska, Gethin Norman, and David Parker. Quantitative analysis with the probabilistic model checker prism. *Electronic Notes in Theoretical Computer Science*, 153(2):5–31, 2006.

[24] R. Lassaigne and S. Peyronnet. Approximate verification of probabilistic systems. *Process Algebra and Probabilistic Methods: Performance Modeling and Verification*, pages 277–295, 2002.

[25] Fei Liu. *Colored Petri Nets for Systems Biology*. PhD thesis, Brandenburg University of Technology Cottbus, 2012.

[26] Fei Liu, Monika Heiner, and Ming Yang. An efficient method for unfolding colored petri nets. In C. Laroque, J. Himmelspach, R. Pasupathy, O. Rose, and A.M. Uhrmacher, editors, *Proceedings of the Winter Simulation Conference*, page 295. Winter Simulation Conference, 2012.

[27] A. Mizera, E. Czeizler, and I. Petre. Self-assembly models of variable resolution. *LNBI Transactions on Computational Systems Biology*, pages 181–203, 2011.

[28] Elaine Murphy, Vincent Danos, Jerome Feret, Jean Krivine, and Russell Harmer. *Elements of Computational Systems Biology*, chapter Rule Based Modelling and Model Refinement, pages 83–114. Wiley Book Series on Bioinformatics. John Wiley & Sons, Inc., 2010.

[29] I. Petre, A. Mizera, C.L. Hyder, A. Meinander, A. Mikhailov, R.I. Morimoto, L. Sistonen, J.E. Eriksson, and R.J. Back. A simple mass-action model for

the eukaryotic heat shock response and its mathematical validation. *Natural Computing*, 10(1):595–612, 2011.

[30] K. Raman and N. Chandra. Systems biology. *Resonance*, 15(2):131–153, 2010.

[31] Wolfgang Reisig and Grzegorz Rozenberg, editors. *Lectures on Petri Nets I: Basic Models, Advances in Petri Nets*, volume 1491 of *Lecture Notes in Computer Science*. Springer, 1998.

[32] Wolfgang Reisig and Grzegorz Rozenberg, editors. *Lectures on Petri Nets II: Applications, Advances in Petri Nets*, volume 1492 of *Lecture Notes in Computer Science*. Springer, 1998.

[33] T.R. Rieger, R.I. Morimoto, and V. Hatzimanikatis. Mathematical modeling of the eukaryotic heat-shock response: Dynamics of the hsp70 promoter. *Biophysical journal*, 88(3):1646–1658, 2005.

[34] C. Rohr, W. Marwan, and M. Heiner. Snoopy - a unifying petri net framework to investigate biomolecular networks. *Bioinformatics*, pages 974–975, 2010.

[35] Y. Shi, D.D. Mosser, and R.I. Morimoto. Molecularchaperones as hsf1-specific transcriptional repressors. *Genes & development*, 12(5):654–666, 1998.

[36] A.M. Smith, W. Xu, Y. Sun, J.R. Faeder, and G.E. Marai. Rulebender: integrated modeling, simulation and visualization for rule-based intracellular biochemistry. *BMC Bioinformatics*, 13(Suppl 8):S3, 2012.

[37] R. Voellmy and F. Boellmann. Chaperone regulation of the heat shock protein response. *Molecular Aspects of the Stress Response: Chaperones, Membranes and Networks*, pages 89–99, 2007.

[38] S.D. Westerheide, J. Anckar, S.M. Stevens Jr, L. Sistonen, and R.I. Morimoto. Stress-inducible regulation of heat shock factor 1 by the deacetylase sirt1. *Science Signalling*, 323(5917):1063–1066, 2009.

[39] W. Xu, A.M. Smith, J.R. Faeder, and G.E. Marai. Rulebender: a visual interface for rule-based modeling. *Bioinformatics*, 27(12):1721–1722, 2011.

Appendix

A The molecular heat shock response model detailing the acetylation status of hsf

Table 4: The list of reactions for the refined model that includes the acetylation status of hsf. For an irreversible reaction q_i, r_i denotes its kinetic rate constant. For a reversible reaction q_i, r_i^+ and r_i^- denote the kinetic rate constants of its 'left-to-right' and 'right-to-left' directions, resp.

Reaction	Reaction number	Kinetic rate constants
$2\,\mathsf{rhsf} \rightleftarrows \mathsf{rhsf}_2$	$[q_1]$	r_1^+, r_1^-
$\mathsf{rhsf} + \mathsf{rhsf}^{(1)} \rightleftarrows \mathsf{rhsf}_2{}^{(1)}$	$[q_2]$	r_2^+, r_2^-
$2\mathsf{rhsf}^{(1)} \rightleftarrows \mathsf{rhsf}_2{}^{(2)}$	$[q_3]$	r_3^+, r_3^-
$\mathsf{rhsf} + \mathsf{rhsf}_2 \rightleftarrows \mathsf{rhsf}_3$	$[q_4]$	r_4^+, r_4^-
$\mathsf{rhsf}^{(1)} + \mathsf{rhsf}_2 \rightleftarrows \mathsf{rhsf}_3{}^{(1)}$	$[q_5]$	r_5^+, r_5^-
$\mathsf{rhsf} + \mathsf{rhsf}_2{}^{(1)} \rightleftarrows \mathsf{rhsf}_3{}^{(1)}$	$[q_6]$	r_6^+, r_6^-
$\mathsf{rhsf}^{(1)} + \mathsf{rhsf}_2{}^{(1)} \rightleftarrows \mathsf{rhsf}_3{}^{(2)}$	$[q_7]$	r_7^+, r_7^-
$\mathsf{rhsf} + \mathsf{rhsf}_2{}^{(2)} \rightleftarrows \mathsf{rhsf}_3{}^{(2)}$	$[q_8]$	r_8^+, r_8^-
$\mathsf{rhsf}^{(1)} + \mathsf{rhsf}_2{}^{(2)} \rightleftarrows \mathsf{rhsf}_3{}^{(3)}$	$[q_9]$	r_9^+, r_9^-
$\mathsf{rhsf}_3 + \mathsf{rhse} \rightleftarrows \mathsf{rhsf}_3\mathsf{:\,rhse}$	$[q_{10}]$	r_{10}^+, r_{10}^-
$\mathsf{rhsf}_3{}^{(1)} + \mathsf{rhse} \rightleftarrows \mathsf{rhsf}_3{}^{(1)}\mathsf{:\,rhse}$	$[q_{11}]$	r_{11}^+, r_{11}^-
$\mathsf{rhsf}_3{}^{(2)} + \mathsf{rhse} \rightleftarrows \mathsf{rhsf}_3{}^{(2)}\mathsf{:\,rhse}$	$[q_{12}]$	r_{12}^+, r_{12}^-
$\mathsf{rhsf}_3{}^{(3)} + \mathsf{rhse} \rightleftarrows \mathsf{rhsf}_3{}^{(3)}\mathsf{:\,rhse}$	$[q_{13}]$	r_{13}^+, r_{13}^-
$\mathsf{rhsf}_3\mathsf{:\,rhse} \rightarrow \mathsf{rhsf}_3\mathsf{:\,rhse} + \mathsf{rhsp}$	$[q_{14}]$	r_{14}
$\mathsf{rhsf}_3{}^{(1)}\mathsf{:\,rhse} \rightarrow \mathsf{rhsf}_3{}^{(1)}\mathsf{:\,rhse} + \mathsf{rhsp}$	$[q_{15}]$	r_{15}
$\mathsf{rhsf}_3{}^{(2)}\mathsf{:\,rhse} \rightarrow \mathsf{rhsf}_3{}^{(2)}\mathsf{:\,rhse} + \mathsf{rhsp}$	$[q_{16}]$	r_{16}
$\mathsf{rhsf}_3{}^{(3)}\mathsf{:\,rhse} \rightarrow \mathsf{rhsf}_3{}^{(3)}\mathsf{:\,rhse} + \mathsf{rhsp}$	$[q_{17}]$	r_{17}
$\mathsf{rhsp} + \mathsf{rhsf} \rightleftarrows \mathsf{rhsp:\,rhsf}$	$[q_{18}]$	r_{18}^+, r_{18}^-
$\mathsf{rhsp} + \mathsf{rhsf}^{(1)} \rightleftarrows \mathsf{rhsp:\,rhsf}^{(1)}$	$[q_{19}]$	r_{19}^+, r_{19}^-
$\mathsf{rhsp} + \mathsf{rhsf}_2 \rightarrow \mathsf{rhsp:\,rhsf} + \mathsf{rhsf}$	$[q_{20}]$	r_{20}
$\mathsf{rhsp} + \mathsf{rhsf}_2{}^{(1)} \rightarrow \mathsf{rhsp:\,rhsf} + \mathsf{rhsf}^{(1)}$	$[q_{21}]$	r_{21}
$\mathsf{rhsp} + \mathsf{rhsf}_2{}^{(1)} \rightarrow \mathsf{rhsp:\,rhsf}^{(1)} + \mathsf{rhsf}$	$[q_{22}]$	r_{22}
$\mathsf{rhsp} + \mathsf{rhsf}_2{}^{(2)} \rightarrow \mathsf{rhsp:\,rhsf}^{(1)} + \mathsf{rhsf}^{(1)}$	$[q_{23}]$	r_{23}
$\mathsf{rhsp} + \mathsf{rhsf}_3 \rightarrow \mathsf{rhsp:\,rhsf} + 2 * \mathsf{rhsf}$	$[q_{24}]$	r_{24}
$\mathsf{rhsp} + \mathsf{rhsf}_3{}^{(1)} \rightarrow \mathsf{rhsp:\,rhsf} + \mathsf{rhsf}^{(1)} + \mathsf{rhsf}$	$[q_{25}]$	r_{25}
$\mathsf{rhsp} + \mathsf{rhsf}_3{}^{(1)} \rightarrow \mathsf{rhsp:\,rhsf}^{(1)} + 2 * \mathsf{rhsf}$	$[q_{26}]$	r_{26}
$\mathsf{rhsp} + \mathsf{rhsf}_3{}^{(2)} \rightarrow \mathsf{rhsp:\,rhsf} + 2\mathsf{rhsf}^{(1)}$	$[q_{27}]$	r_{27}

Table 4: The list of reactions for the refined model - Continued.

$\mathsf{rhsp} + \mathsf{rhsf_3}^{(2)} \rightarrow \mathsf{rhsp{:}\ rhsf}^{(1)} + \mathsf{rhsf}^{(1)} + \mathsf{rhsf}$	$[q_{28}]$	r_{28}
$\mathsf{rhsp} + \mathsf{rhsf_3}^{(3)} \rightarrow \mathsf{rhsp{:}\ rhsf}^{(1)} + 2\mathsf{rhsf}^{(1)}$	$[q_{29}]$	r_{29}
$\mathsf{rhsp} + \mathsf{rhsf_3{:}\ rhse} \rightarrow \mathsf{rhsp{:}\ rhsf} + 2\,\mathsf{rhsf} + \mathsf{rhse}$	$[q_{30}]$	r_{30}
$\mathsf{rhsp} + \mathsf{rhsf_3}^{(1)}\mathsf{{:}\ rhse} \rightarrow \mathsf{rhsp{:}\ rhsf}^{(1)} + 2\,\mathsf{rhsf} + \mathsf{rhse}$	$[q_{31}]$	r_{31}
$\mathsf{rhsp} + \mathsf{rhsf_3}^{(1)}\mathsf{{:}\ rhse} \rightarrow \mathsf{rhsp{:}\ rhsf} + \mathsf{rhsf}^{(1)} + \mathsf{rhsf} + \mathsf{rhse}$	$[q_{32}]$	r_{32}
$\mathsf{rhsp} + \mathsf{rhsf_3}^{(2)}\mathsf{{:}\ rhse} \rightarrow \mathsf{rhsp{:}\ rhsf}^{(1)} + \mathsf{rhsf}^{(1)} + \mathsf{rhsf} + \mathsf{rhse}$	$[q_{33}]$	r_{33}
$\mathsf{rhsp} + \mathsf{rhsf_3}^{(2)}\mathsf{{:}\ rhse} \rightarrow \mathsf{rhsp{:}\ rhsf} + 2\mathsf{rhsf}^{(1)} + \mathsf{rhse}$	$[q_{34}]$	r_{34}
$\mathsf{rhsp} + \mathsf{rhsf_3}^{(3)}\mathsf{{:}\ rhse} \rightarrow \mathsf{rhsp{:}\ rhsf}^{(1)} + 2\mathsf{rhsf}^{(1)} + \mathsf{rhse}$	$[q_{35}]$	r_{35}
$\mathsf{rhsp} \rightarrow \emptyset$	$[q_{36}]$	r_{36}
$\mathsf{rprot} \rightarrow \mathsf{rmfp}$	$[q_{37}]$	r_{37}
$\mathsf{rhsp} + \mathsf{rmfp} \rightleftarrows \mathsf{rhsp{:}\ rmfp}$	$[q_{38}]$	r_{38}^{+}, r_{38}^{-}
$\mathsf{rhsp{:}\ rmfp} \rightarrow \mathsf{rhsp} + \mathsf{rprot}$	$[q_{39}]$	r_{39}

B The ODE-based models for the heat shock response

Table 5: The numerical setup of the acetylation-refined heat shock response model.

$r_1^+ = k_1^+;$	$r_8^+ = k_2^+;$	$r_{16} = k_4;$	$r_{28} = k_7/2;$
$r_1^- = k_1^-;$	$r_8^- = k_2^-/2;$	$r_{17} = k_4;$	$r_{29} = k_7;$
$r_2^+ = 2 \cdot k_1^+;$	$r_9^+ = k_2^+;$	${r_{18}}^+ = k_5^+;$	$r_{30} = k_8;$
$r_2^- = k_1^-;$	$r_9^- = k_2^-;$	${r_{18}}^- = k_5^-;$	$r_{31} = k_8/2;$
$r_3^+ = k_1^+;$	${r_{10}}^+ = k_3^+;$	${r_{19}}^+ = k_5^+;$	$r_{32} = k_8/2;$
$r_3^- = k_1^-;$	${r_{10}}^- = k_3^-;$	${r_{19}}^- = k_5^-;$	$r_{33} = k_8/2;$
$r_4^+ = k_2^+;$	${r_{11}}^+ = k_3^+;$	$r_{20} = k_6;$	$r_{34} = k_8/2;$
$r_4^- = k_2^-;$	${r_{11}}^- = k_3^-;$	$r_{21} = k_6/2;$	$r_{35} = k_8;$
$r_5^+ = k_2^+;$	${r_{12}}^+ = k_3^+;$	$r_{22} = k_6/2;$	$r_{36} = k_9;$
$r_5^- = k_2^-/2;$	${r_{12}}^- = k_3^-;$	$r_{23} = k_6;$	$r_{37} = \Phi_T;$
$r_6^+ = k_2^+;$	${r_{13}}^+ = k_3^+;$	$r_{24} = k_7;$	$r_{38}^- = {k_{11}}^-;$
$r_6^- = k_2^-/2;$	${r_{13}}^- = k_3^-;$	$r_{25} = k_7/2;$	$r_{38}^+ = {k_{11}}^+;$
$r_7^+ = k_2^+;$	$r_{14} = k_4;$	$r_{26} = k_7/2;$	$r_{39} = k_{12}$
$r_7^- = k_2^-/2;$	$r_{15} = k_4;$	$r_{27} = k_7/2;$	

Table 6: The ODE model for the basic heat shock response model proposed in [29].

$$
\begin{aligned}
d[\mathsf{hsf}]/dt &= -2k_1^+[\mathsf{hsf}]^2 + 2k_1^-[\mathsf{hsf}_2] - k_2^+[\mathsf{hsf}][\mathsf{hsf}_2] + k_2^-[\mathsf{hsf}_3] \\
&\quad -k_5^+[\mathsf{hsf}][\mathsf{hsp}] + k_5^-[\mathsf{hsp{:}\ hsf}] + k_6[\mathsf{hsf}_2][\mathsf{hsp}] \\
&\quad +2k_7[\mathsf{hsf}_3][\mathsf{hsp}] + 2k_8[\mathsf{hsf_3{:}\ hse}][\mathsf{hsp}] \\
d[\mathsf{hsf}_2]/dt &= k_1^+[\mathsf{hsf}]^2 - k_1^-[\mathsf{hsf}_2] - k_2^+[\mathsf{hsf}][\mathsf{hsf}_2] + k_2^-[\mathsf{hsf}_3] \\
&\quad -k_6[\mathsf{hsf}_2][\mathsf{hsp}] \\
d[\mathsf{hsf}_3]/dt &= k_2^+[\mathsf{hsf}][\mathsf{hsf}_2] - k_2^-[\mathsf{hsf}_3] - k_3^+[\mathsf{hsf}_3][\mathsf{hse}] + k_3^-[\mathsf{hsf_3{:}\ hse}] \\
&\quad -k_7[\mathsf{hsf}_3][\mathsf{hsp}] \\
d[\mathsf{hse}]/dt &= -k_3^+[\mathsf{hsf}_3][\mathsf{hse}] + k_3^-[\mathsf{hsf_3{:}\ hse}] + k_8[\mathsf{hsf_3{:}\ hse}][\mathsf{hsp}] \\
d[\mathsf{hsf_3{:}\ hse}]/dt &= k_3^+[\mathsf{hsf}_3][\mathsf{hse}] - k_3^-[\mathsf{hsf_3{:}\ hse}] - k_8[\mathsf{hsf_3{:}\ hse}][\mathsf{hsp}] \\
d[\mathsf{hsp}]/dt &= k_4[\mathsf{hsf_3{:}\ hse}] - k_5^+[\mathsf{hsf}][\mathsf{hsp}] + k_5^-[\mathsf{hsp{:}\ hsf}] - k_6[\mathsf{hsf}_2][\mathsf{hsp}] \\
&\quad -k_7[\mathsf{hsf}_3][\mathsf{hsp}] - k_8[\mathsf{hsf_3{:}\ hse}][\mathsf{hsp}] - k_{11}^+[\mathsf{hsp}][\mathsf{mfp}] \\
&\quad +(k_{11}^- + k_{12})[\mathsf{hsp{:}\ mfp}] - k_9[\mathsf{hsp}] \\
d[\mathsf{hsp{:}\ hsf}]/dt &= k_5^+[\mathsf{hsf}][\mathsf{hsp}] - k_5^-[\mathsf{hsp{:}\ hsf}] + k_6[\mathsf{hsf}_2][\mathsf{hsp}] \\
&\quad +k_7[\mathsf{hsf}_3][\mathsf{hsp}] + k_8[\mathsf{hsf_3{:}\ hse}][\mathsf{hsp}] \\
d[\mathsf{mfp}]/dt &= \phi_T[\mathsf{prot}] - k_{11}^+[\mathsf{hsp}][\mathsf{mfp}] + k_{11}^-[\mathsf{hsp{:}\ mfp}] \\
d[\mathsf{hsp{:}\ mfp}]/dt &= k_{11}^+[\mathsf{hsp}][\mathsf{mfp}] - (k_{11}^- + k_{12})[\mathsf{hsp{:}\ mfp}] \\
d[\mathsf{prot}]/dt &= -\phi_T[\mathsf{prot}] + k_{12}[\mathsf{hsp{:}\ mfp}]
\end{aligned}
$$

Table 7: The ODE model for the acetylation-refined heat shock response model.

$$
\begin{aligned}
d[\mathsf{rhsf}]/dt &= -2r_1^+[\mathsf{rhsf}]^2 + 2r_1^-[\mathsf{rhsf_2}] - r_2^+[\mathsf{rhsf}][\mathsf{rhsf}^{(1)}] + r_2^-[\mathsf{rhsf_2}^{(1)}] \\
&\quad -r_4{}^+[\mathsf{rhsf}][\mathsf{rhsf_2}] + r_4{}^-[\mathsf{rhsf_3}] - r_6{}^+[\mathsf{rhsf}][\mathsf{rhsf_2}^{(1)}] + r_6{}^-[\mathsf{rhsf_3}^{(1)}] \\
&\quad -r_8{}^+[\mathsf{rhsf}][\mathsf{rhsf_2}^{(2)}] + r_8{}^-[\mathsf{rhsf_3}^{(2)}] - r_{18}{}^+[\mathsf{rhsp}][\mathsf{rhsf}] \\
&\quad +r_{18}{}^-[\mathsf{rhsp{:}\,rhsf}] + r_{20}[\mathsf{rhsp}][\mathsf{rhsf_2}] + r_{22}[\mathsf{rhsp}][\mathsf{rhsf_2}^{(1)}] \\
&\quad +2r_{24}[\mathsf{rhsp}][\mathsf{rhsf_3}] + r_{25}[\mathsf{rhsp}][\mathsf{rhsf_3}^{(1)}] + 2r_{26}[\mathsf{rhsp}][\mathsf{rhsf_3}^{(1)}] \\
&\quad +r_{28}[\mathsf{rhsp}][\mathsf{rhsf_3}^{(2)}] + 2r_{30}[\mathsf{rhsp}][\mathsf{rhsf_3{:}\,rhse}] \\
&\quad +2r_{31}[\mathsf{rhsp}][\mathsf{rhsf_3}^{(1)}{:}\,\mathsf{rhse}] + r_{32}[\mathsf{rhsp}][\mathsf{rhsf_3}^{(1)}{:}\,\mathsf{rhse}] \\
&\quad +r_{33}[\mathsf{rhsp}][\mathsf{rhsf_3}^{(2)}{:}\,\mathsf{rhse}] \\
d[\mathsf{rhsf}^{(1)}]/dt &= -r_2^+[\mathsf{rhsf}][\mathsf{rhsf}^{(1)}] + r_2^-[\mathsf{rhsf_2}^{(1)}] - 2r_3{}^+[\mathsf{rhsf}^{(1)}]^2 \\
&\quad +2r_3{}^-[\mathsf{rhsf_2}^{(2)}] - r_5{}^+[\mathsf{rhsf}^{(1)}][\mathsf{rhsf_2}] + r_5{}^-[\mathsf{rhsf_3}^{(1)}] \\
&\quad -r_7{}^+[\mathsf{rhsf}^{(1)}][\mathsf{rhsf_2}^{(1)}] + r_7{}^-[\mathsf{rhsf_3}^{(2)}] - r_9{}^+[\mathsf{rhsf}^{(1)}][\mathsf{rhsf_2}^{(2)}] \\
&\quad +r_9{}^-[\mathsf{rhsf_3}^{(3)}] - r_{19}{}^+[\mathsf{rhsp}][\mathsf{rhsf}^{(1)}] + r_{19}{}^-[\mathsf{rhsp{:}\,rhsf}^{(1)}] \\
&\quad +r_{21}[\mathsf{rhsp}][\mathsf{rhsf_2}^{(1)}] + r_{23}[\mathsf{rhsp}][\mathsf{rhsf_2}^{(2)}] + r_{25}[\mathsf{rhsp}][\mathsf{rhsf_3}^{(1)}] \\
&\quad +2r_{27}[\mathsf{rhsp}][\mathsf{rhsf_3}^{(2)}] + r_{28}[\mathsf{rhsp}][\mathsf{rhsf_3}^{(2)}] + 2r_{29}[\mathsf{rhsp}][\mathsf{rhsf_3}^{(3)}] \\
&\quad +r_{32}[\mathsf{rhsp}][\mathsf{rhsf_3}^{(1)}{:}\,\mathsf{rhse}] + r_{33}[\mathsf{rhsp}][\mathsf{rhsf_3}^{(2)}{:}\,\mathsf{rhse}] \\
&\quad +2r_{34}[\mathsf{rhsp}][\mathsf{rhsf_3}^{(2)}{:}\,\mathsf{rhse}] + 2r_{35}[\mathsf{rhsp}][\mathsf{rhsf_3}^{(3)}{:}\,\mathsf{rhse}] \\
d[\mathsf{rhsf_2}]/dt &= r_1^+[\mathsf{rhsf}]^2 - r_1^-[\mathsf{rhsf_2}] - r_4^+[\mathsf{rhsf}][\mathsf{rhsf_2}] + r_4^-[\mathsf{rhsf_3}] \\
&\quad -r_5^+[\mathsf{rhsf}^{(1)}][\mathsf{rhsf_2}] + r_5^-[\mathsf{rhsf_3}^{(1)}] - r_{20}[\mathsf{rhsp}][\mathsf{rhsf_2}] \\
d[\mathsf{rhsf_2}^{(1)}]/dt &= r_2^+[\mathsf{rhsf}][\mathsf{rhsf}^{(1)}] - r_2^-[\mathsf{rhsf_2}^{(1)}] - r_6^+[\mathsf{rhsf}][\mathsf{rhsf_2}^{(1)}] \\
&\quad +r_6^-[\mathsf{rhsf_3}^{(1)}] - r_7^+[\mathsf{rhsf}^{(1)}][\mathsf{rhsf_2}^{(1)}] + r_7^-[\mathsf{rhsf_3}^{(2)}] \\
&\quad -r_{21}[\mathsf{rhsp}][\mathsf{rhsf_2}^{(1)}] - r_{22}[\mathsf{rhsp}][\mathsf{rhsf_2}^{(1)}] \\
d[\mathsf{rhsf_2}^{(2)}]/dt &= r_3^+[\mathsf{rhsf}^{(1)}]^2 - r_3^-[\mathsf{rhsf_2}^{(2)}] - r_8^+[\mathsf{rhsf}][\mathsf{rhsf_2}^{(2)}] \\
&\quad +r_8^-[\mathsf{rhsf_3}^{(2)}] - r_9^+[\mathsf{rhsf}^{(1)}][\mathsf{rhsf_2}^{(2)}] + r_9^-[\mathsf{rhsf_3}^{(3)}] \\
&\quad -r_{23}[\mathsf{rhsp}][\mathsf{rhsf_2}^{(2)}] \\
d[\mathsf{rhsf_3}]/dt &= r_4^+[\mathsf{rhsf}][\mathsf{rhsf_2}] - r_4^-[\mathsf{rhsf_3}] - r_{10}^+[\mathsf{rhsf_3}][\mathsf{rhse}] \\
&\quad +r_{10}^-[\mathsf{rhsf_3{:}\,rhse}] - r_{24}[\mathsf{rhsp}][\mathsf{rhsf_3}] \\
d[\mathsf{rhsf_3}^{(1)}]/dt &= r_5^+[\mathsf{rhsf}^{(1)}][\mathsf{rhsf_2}] - r_5^-[\mathsf{rhsf_3}^{(1)}] + r_6^+[\mathsf{rhsf}][\mathsf{rhsf_2}^{(1)}] \\
&\quad -r_6^-[\mathsf{rhsf_3}^{(1)}] - r_{11}^+[\mathsf{rhsf_3}^{(1)}][\mathsf{rhse}] + r_{11}^-[\mathsf{rhsf_3}^{(1)}{:}\,\mathsf{rhse}] \\
&\quad -r_{25}[\mathsf{rhsp}][\mathsf{rhsf_3}^{(1)}] - r_{26}[\mathsf{rhsp}][\mathsf{rhsf_3}^{(1)}] \\
d[\mathsf{rhsf_3}^{(2)}]/dt &= r_7^+[\mathsf{rhsf}^{(1)}][\mathsf{rhsf_2}^{(1)}] - r_7^-[\mathsf{rhsf_3}^{(2)}] + r_8^+[\mathsf{rhsf}][\mathsf{rhsf_2}^{(2)}] \\
&\quad -r_8^-[\mathsf{rhsf_3}^{(2)}] - r_{12}^+[\mathsf{rhsf_3}^{(2)}][\mathsf{rhse}] + r_{12}^-[\mathsf{rhsf_3}^{(2)}{:}\,\mathsf{rhse}] \\
&\quad -r_{27}[\mathsf{rhsp}][\mathsf{rhsf_3}^{(2)}] - r_{28}[\mathsf{rhsp}][\mathsf{rhsf_3}^{(2)}] \\
d[\mathsf{rhsf_3}^{(3)}]/dt &= r_9^+[\mathsf{rhsf}^{(1)}][\mathsf{rhsf_2}^{(2)}] - r_9^-[\mathsf{rhsf_3}^{(3)}] - r_{13}^+[\mathsf{rhsf_3}^{(3)}][\mathsf{rhse}] \\
&\quad +r_{13}^-[\mathsf{rhsf_3}^{(3)}{:}\,\mathsf{rhse}] - r_{29}[\mathsf{rhsp}][\mathsf{rhsf_3}^{(3)}] \\
d[\mathsf{rhse}]/dt &= -r_{10}^+[\mathsf{rhsf_3}][\mathsf{rhse}] + r_{10}^-[\mathsf{rhsf_3{:}\,rhse}] - r_{11}^+[\mathsf{rhsf_3}^{(1)}][\mathsf{rhse}] \\
&\quad +r_{11}^-[\mathsf{rhsf_3}^{(1)}{:}\,\mathsf{rhse}] - r_{12}^+[\mathsf{rhsf_3}^{(2)}][\mathsf{rhse}] + r_{12}^-[\mathsf{rhsf_3}^{(2)}{:}\,\mathsf{rhse}] \\
&\quad -r_{13}^+[\mathsf{rhsf_3}^{(3)}][\mathsf{rhse}] + r_{13}^-[\mathsf{rhsf_3}^{(3)}{:}\,\mathsf{rhse}] + r_{30}[\mathsf{rhsp}][\mathsf{rhsf_3{:}\,rhse}]
\end{aligned}
$$

Table 7: The ODE model for the acetylation-refined heat shock response model - Continued.

$$
\begin{aligned}
&+r_{31}[\mathsf{rhsp}][\mathsf{rhsf_3}^{(1)}\colon \mathsf{rhse}] + r_{32}[\mathsf{rhsp}][\mathsf{rhsf_3}^{(1)}\colon \mathsf{rhse}]\\
&+r_{33}[\mathsf{rhsp}][\mathsf{rhsf_3}^{(2)}\colon \mathsf{rhse}] + r_{34}[\mathsf{rhsp}][\mathsf{rhsf_3}^{(2)}\colon \mathsf{rhse}]\\
&+r_{35}[\mathsf{rhsp}][\mathsf{rhsf_3}^{(3)}\colon \mathsf{rhse}]\\
d[\mathsf{rhsf_3}\colon \mathsf{rhse}]/dt &= r_{10}^{+}[\mathsf{rhsf_3}][\mathsf{rhse}] - r_{10}^{-}[\mathsf{rhsf_3}\colon \mathsf{rhse}]\\
&-r_{30}[\mathsf{rhsp}][\mathsf{rhsf_3}\colon \mathsf{rhse}]\\
d[\mathsf{rhsf_3}^{(1)}\colon \mathsf{rhse}]/dt &= r_{11}^{+}[\mathsf{rhsf_3}^{(1)}][\mathsf{rhse}] - r_{11}^{-}[\mathsf{rhsf_3}^{(1)}\colon \mathsf{rhse}]\\
&-r_{31}[\mathsf{rhsp}][\mathsf{rhsf_3}^{(1)}\colon \mathsf{rhse}] - r_{32}[\mathsf{rhsp}][\mathsf{rhsf_3}^{(1)}\colon \mathsf{rhse}]\\
d[\mathsf{rhsf_3}^{(2)}\colon \mathsf{rhse}]/dt &= r_{12}^{+}[\mathsf{rhsf_3}^{(2)}][\mathsf{rhse}] - r_{12}^{-}[\mathsf{rhsf_3}^{(2)}\colon \mathsf{rhse}]\\
&-r_{33}[\mathsf{rhsp}][\mathsf{rhsf_3}^{(2)}\colon \mathsf{rhse}] - r_{34}[\mathsf{rhsp}][\mathsf{rhsf_3}^{(2)}\colon \mathsf{rhse}]\\
d[\mathsf{rhsf_3}^{(3)}\colon \mathsf{rhse}]/dt &= r_{13}^{+}[\mathsf{rhsf_3}^{(3)}][\mathsf{rhse}] - r_{13}^{-}[\mathsf{rhsf_3}^{(3)}\colon \mathsf{rhse}]\\
&-r_{35}[\mathsf{rhsp}][\mathsf{rhsf_3}^{(3)}\colon \mathsf{rhse}]\\
d[\mathsf{rhsp}]/dt &= r_{14}[\mathsf{rhsf_3}\colon \mathsf{rhse}] + r_{15}[\mathsf{rhsf_3}^{(1)}\colon \mathsf{rhse}] + r_{16}[\mathsf{rhsf_3}^{(2)}\colon \mathsf{rhse}]\\
&+r_{17}[\mathsf{rhsf_3}^{(3)}\colon \mathsf{rhse}] - r_{18}^{+}[\mathsf{rhsp}][\mathsf{rhsf}] + r_{18}^{-}[\mathsf{rhsp}\colon \mathsf{rhsf}]\\
&-r_{19}^{+}[\mathsf{rhsp}][\mathsf{rhsf}^{(1)}] + r_{19}^{-}[\mathsf{rhsp}\colon \mathsf{rhsf}^{(1)}] - r_{20}[\mathsf{rhsp}][\mathsf{rhsf_2}]\\
&-r_{21}[\mathsf{rhsp}][\mathsf{rhsf_2}^{(1)}] - r_{22}[\mathsf{rhsp}][\mathsf{rhsf_2}^{(1)}] - r_{23}[\mathsf{rhsp}][\mathsf{rhsf_2}^{(2)}]\\
&-r_{24}[\mathsf{rhsp}][\mathsf{rhsf_3}] - r_{25}[\mathsf{rhsp}][\mathsf{rhsf_3}^{(1)}] - r_{26}[\mathsf{rhsp}][\mathsf{rhsf_3}^{(1)}]\\
&-r_{27}[\mathsf{rhsp}][\mathsf{rhsf_3}^{(2)}] - r_{28}[\mathsf{rhsp}][\mathsf{rhsf_3}^{(2)}] - r_{29}[\mathsf{rhsp}][\mathsf{rhsf_3}^{(3)}]\\
&-r_{30}[\mathsf{rhsp}][\mathsf{rhsf_3}\colon \mathsf{rhse}] - r_{31}[\mathsf{rhsp}][\mathsf{rhsf_3}^{(1)}\colon \mathsf{rhse}]\\
&-r_{32}[\mathsf{rhsp}][\mathsf{rhsf_3}^{(1)}\colon \mathsf{rhse}] - r_{33}[\mathsf{rhsp}][\mathsf{rhsf_3}^{(2)}\colon \mathsf{rhse}]\\
&-r_{34}[\mathsf{rhsp}][\mathsf{rhsf_3}^{(2)}\colon \mathsf{rhse}] - r_{35}[\mathsf{rhsp}][\mathsf{rhsf_3}^{(3)}\colon \mathsf{rhse}] - r_{36}[\mathsf{rhsp}]\\
&-r_{38}^{+}[\mathsf{rhsp}][\mathsf{rmfp}] + r_{38}^{-}[\mathsf{rhsp}\colon \mathsf{rmfp}] + r_{39}[\mathsf{rhsp}][\mathsf{rmfp}]\\
d[\mathsf{rhsp}\colon \mathsf{rhsf}]/dt &= r_{18}^{+}[\mathsf{rhsp}][\mathsf{rhsf}] - r_{18}^{-}[\mathsf{rhsp}\colon \mathsf{rhsf}] + r_{20}[\mathsf{rhsp}][\mathsf{rhsf_2}]\\
&+r_{21}[\mathsf{rhsp}][\mathsf{rhsf_2}^{(1)}] + r_{24}[\mathsf{rhsp}][\mathsf{rhsf_3}]\\
&+r_{25}[\mathsf{rhsp}][\mathsf{rhsf_3}^{(1)}] + r_{27}[\mathsf{rhsp}][\mathsf{rhsf_3}^{(2)}]\\
&+r_{30}[\mathsf{rhsp}][\mathsf{rhsf_3}\colon \mathsf{rhse}] + r_{32}[\mathsf{rhsp}][\mathsf{rhsf_3}^{(1)}\colon \mathsf{rhse}]\\
&+r_{34}[\mathsf{rhsp}][\mathsf{rhsf_3}^{(2)}\colon \mathsf{rhse}]\\
d[\mathsf{rhsp}\colon \mathsf{rhsf}^{(1)}]/dt &= {r_{19}}^{+}[\mathsf{rhsp}][\mathsf{rhsf}^{(1)}] - {r_{19}}^{-}[\mathsf{rhsp}\colon \mathsf{rhsf}^{(1)}]\\
&+r_{22}[\mathsf{rhsp}][\mathsf{rhsf_2}^{(1)}] + r_{23}[\mathsf{rhsp}][\mathsf{rhsf_2}^{(2)}]\\
&+r_{26}[\mathsf{rhsp}][\mathsf{rhsf_3}^{(1)}] + r_{28}[\mathsf{rhsp}][\mathsf{rhsf_3}^{(2)}]\\
&+r_{29}[\mathsf{rhsp}][\mathsf{rhsf_3}^{(3)}] + r_{31}[\mathsf{rhsp}][\mathsf{rhsf_3}^{(1)}\colon \mathsf{rhse}]\\
&+r_{33}[\mathsf{rhsp}][\mathsf{rhsf_3}^{(2)}\colon \mathsf{rhse}] + r_{35}[\mathsf{rhsp}][\mathsf{rhsf_3}^{(3)}\colon \mathsf{rhse}]\\
d[\mathsf{rhsp}\colon \mathsf{rmfp}]/dt &= r_{38}^{+}[\mathsf{rhsp}][\mathsf{rmfp}] - (r_{38}^{-} + r_{39})[\mathsf{rhsp}\colon \mathsf{rmfp}]\\
d[\mathsf{rmfp}]/dt &= r_{37}[\mathsf{rprot}] - r_{38}^{+}[\mathsf{rhsp}][\mathsf{rmfp}] + r_{38}^{-}[\mathsf{rhsp}\colon \mathsf{rmfp}]\\
d[\mathsf{rprot}]/dt &= -r_{37}[\mathsf{rprot}] + r_{39}[\mathsf{rhsp}\colon \mathsf{rmfp}]
\end{aligned}
$$

Table 8: The system of ODEs corresponding to Rhsf, $\mathsf{Rhsf_2}$, $\mathsf{Rhsf_3}$, $\mathsf{Rhsf_3}$: Rhse, and Rhsp: Rhsf in the refined model

$$
\begin{aligned}
d[\mathsf{Rhsf}]/dt &= -2(r_1^+[\mathsf{rhsf}]^2 + r_2^+[\mathsf{rhsf}][\mathsf{rhsf}^{(1)}] + r_3{}^+[\mathsf{rhsf}^{(1)}]^2) + 2(r_1^-[\mathsf{rhsf_2}] \\
&\quad + r_2^-[\mathsf{rhsf_2}{}^{(1)}] + r_3{}^-[\mathsf{rhsf_2}{}^{(2)}]) - (r_4{}^+[\mathsf{rhsf}][\mathsf{rhsf_2}] \\
&\quad + r_6{}^+[\mathsf{rhsf}][\mathsf{rhsf_2}{}^{(1)}] + r_8{}^+[\mathsf{rhsf}][\mathsf{rhsf_2}{}^{(2)}] + r_5{}^+[\mathsf{rhsf}^{(1)}][\mathsf{rhsf_2}] \\
&\quad + r_7{}^+[\mathsf{rhsf}^{(1)}][\mathsf{rhsf_2}{}^{(1)}] + r_9{}^+[\mathsf{rhsf}^{(1)}][\mathsf{rhsf_2}{}^{(2)}]) + (r_4{}^-[\mathsf{rhsf_3}] + (r_5{}^- \\
&\quad + r_6{}^-)[\mathsf{rhsf_3}{}^{(1)}] + (r_7{}^- + r_8{}^-)[\mathsf{rhsf_3}{}^{(2)}] + r_9{}^-[\mathsf{rhsf_3}{}^{(3)}]) \\
&\quad - [\mathsf{rhsp}](r_{18}{}^+[\mathsf{rhsf}] + r_{19}{}^+[\mathsf{rhsf}^{(1)}]) + (r_{18}{}^-[\mathsf{rhsp{:}\ rhsf}] \\
&\quad + r_{19}{}^-[\mathsf{rhsp{:}\ rhsf}^{(1)}]) + [\mathsf{rhsp}](r_{20}[\mathsf{rhsf_2}] + (r_{21} + r_{22})[\mathsf{rhsf_2}{}^{(1)}] \\
&\quad + r_{23}[\mathsf{rhsf_2}{}^{(2)}]) + 2[\mathsf{rhsp}](r_{24}[\mathsf{rhsf_3}] + (r_{25} + r_{26})[\mathsf{rhsf_3}{}^{(1)}] + (r_{27} \\
&\quad + r_{28})[\mathsf{rhsf_3}{}^{(2)}] + r_{29}[\mathsf{rhsf_3}{}^{(3)}]) + 2[\mathsf{rhsp}](r_{30}[\mathsf{rhsf_3{:}\ rhse}] \\
&\quad + (r_{31} + r_{32})[\mathsf{rhsf_3}{}^{(1)}\mathsf{{:}\ rhse}] + (r_{33} + r_{34})[\mathsf{rhsf_3}{}^{(2)}\mathsf{{:}\ rhse}] \\
&\quad + r_{35}[\mathsf{rhsf_3}{}^{(3)}\mathsf{{:}\ rhse}]) \\
d[\mathsf{Rhsf_2}]/dt &= (r_1^+[\mathsf{rhsf}]^2 + r_2^+[\mathsf{rhsf}][\mathsf{rhsf}^{(1)}] + r_3^+[\mathsf{rhsf}^{(1)}]^2) - (r_1^-[\mathsf{rhsf_2}] \\
&\quad + r_2^-[\mathsf{rhsf_2}{}^{(1)}] + r_3^-[\mathsf{rhsf_2}{}^{(2)}]) - (r_4^+[\mathsf{rhsf}][\mathsf{rhsf_2}] + r_6^+[\mathsf{rhsf}][\mathsf{rhsf_2}{}^{(1)}] \\
&\quad + r_8^+[\mathsf{rhsf}][\mathsf{rhsf_2}{}^{(2)}] + r_5^+[\mathsf{rhsf}^{(1)}][\mathsf{rhsf_2}] + r_7^+[\mathsf{rhsf}^{(1)}][\mathsf{rhsf_2}{}^{(1)}] \\
&\quad + r_9^+[\mathsf{rhsf}^{(1)}][\mathsf{rhsf_2}{}^{(2)}]) + (r_4^-[\mathsf{rhsf_3}] + (r_5^- + r_6^-)[\mathsf{rhsf_3}{}^{(1)}]) \\
&\quad + (r_7^- + r_8^-)[\mathsf{rhsf_3}{}^{(2)}] + r_9^-[\mathsf{rhsf_3}{}^{(3)}]) - [\mathsf{rhsp}](r_{20}[\mathsf{rhsf_2}] \\
&\quad + (r_{21} + r_{22})[\mathsf{rhsf_2}{}^{(1)}] + r_{23}[\mathsf{rhsf_2}{}^{(2)}]) \\
d[\mathsf{Rhsf_3}]/dt &= (r_4^+[\mathsf{rhsf}][\mathsf{rhsf_2}] + r_6^+[\mathsf{rhsf}][\mathsf{rhsf_2}{}^{(1)}] + r_8^+[\mathsf{rhsf}][\mathsf{rhsf_2}{}^{(2)}] \\
&\quad + r_5^+[\mathsf{rhsf}^{(1)}][\mathsf{rhsf_2}] + r_7^+[\mathsf{rhsf}^{(1)}][\mathsf{rhsf_2}{}^{(1)}] + r_9^+[\mathsf{rhsf}^{(1)}][\mathsf{rhsf_2}{}^{(2)}]) \\
&\quad - (r_4^-[\mathsf{rhsf_3}] + (r_5^- + r_6^-)[\mathsf{rhsf_3}{}^{(1)}] + (r_7^- + r_8^-)[\mathsf{rhsf_3}{}^{(2)}] \\
&\quad + r_9^-[\mathsf{rhsf_3}{}^{(3)}]) - [\mathsf{rhse}](r_{10}^+[\mathsf{rhsf_3}] + r_{11}^+[\mathsf{rhsf_3}{}^{(1)}] + r_{12}^+[\mathsf{rhsf_3}{}^{(2)}] \\
&\quad + r_{13}^+[\mathsf{rhsf_3}{}^{(3)}]) + (r_{10}^-[\mathsf{rhsf_3{:}\ rhse}] + r_{11}^-[\mathsf{rhsf_3}{}^{(1)}\mathsf{{:}\ rhse}] \\
&\quad + r_{12}^-[\mathsf{rhsf_3}{}^{(2)}\mathsf{{:}\ rhse}] + r_{13}^-[\mathsf{rhsf_3}{}^{(3)}\mathsf{{:}\ rhse}]) - [\mathsf{rhsp}](r_{24}[\mathsf{rhsf_3}] \\
&\quad + (r_{25} + r_{26})[\mathsf{rhsf_3}{}^{(1)}] + (r_{27} + r_{28})[\mathsf{rhsf_3}{}^{(2)}] + r_{29}[\mathsf{rhsf_3}{}^{(3)}]) \\
d[\mathsf{Rhsf_3{:}\ Rhse}]/dt &= [\mathsf{rhse}](r_{10}^+[\mathsf{rhsf_3}] + r_{11}^+[\mathsf{rhsf_3}{}^{(1)}] + r_{12}^+[\mathsf{rhsf_3}{}^{(2)}] \\
&\quad + r_{13}^+[\mathsf{rhsf_3}{}^{(3)}]) - (r_{10}^-[\mathsf{rhsf_3{:}\ rhse}] + r_{11}^-[\mathsf{rhsf_3}{}^{(1)}\mathsf{{:}\ rhse}] \\
&\quad + r_{12}^-[\mathsf{rhsf_3}{}^{(2)}\mathsf{{:}\ rhse}] + r_{13}^-[\mathsf{rhsf_3}{}^{(3)}\mathsf{{:}\ rhse}]) - [\mathsf{rhsp}](r_{30}[\mathsf{rhsf_3{:}\ rhse}] \\
&\quad + (r_{31} + r_{32})[\mathsf{rhsf_3}{}^{(1)}\mathsf{{:}\ rhse}] + (r_{33} + r_{34})[\mathsf{rhsf_3}{}^{(2)}\mathsf{{:}\ rhse}] \\
&\quad + r_{35}[\mathsf{rhsf_3}{}^{(3)}\mathsf{{:}\ rhse}]) \\
d[\mathsf{Rhsp{:}\ Rhsf}]/dt &= [\mathsf{rhsp}](r_{18}^+[\mathsf{rhsf}] + r_{19}{}^+[\mathsf{rhsf}^{(1)}]) - (r_{18}^-[\mathsf{rhsp{:}\ rhsf}] \\
&\quad + r_{19}{}^-[\mathsf{rhsp{:}\ rhsf}^{(1)}]) + [\mathsf{rhsp}](r_{20}[\mathsf{rhsf_2}] + (r_{21} + r_{22})[\mathsf{rhsf_2}{}^{(1)}] \\
&\quad + r_{23}[\mathsf{rhsf_2}{}^{(2)}]) + [\mathsf{rhsp}](r_{24}[\mathsf{rhsf_3}] + (r_{25} + r_{26})[\mathsf{rhsf_3}{}^{(1)}] \\
&\quad + (r_{27} + r_{28})[\mathsf{rhsf_3}{}^{(2)}] + r_{29}[\mathsf{rhsf_3}{}^{(3)}]) \\
&\quad + [\mathsf{rhsp}](r_{30}[\mathsf{rhsf_3{:}\ rhse}] + (r_{31} + r_{32})[\mathsf{rhsf_3}{}^{(1)}\mathsf{{:}\ rhse}] \\
&\quad (r_{33} + r_{34})[\mathsf{rhsf_3}{}^{(2)}\mathsf{{:}\ rhse}] + r_{35}[\mathsf{rhsf_3}{}^{(3)}\mathsf{{:}\ rhse}])
\end{aligned}
$$

C The Petri net model analysis

Figure 8: Snoopy representation of the transition-focused refined heat shock response model. The network is similar to the basic model network. We include here the information about each place's color set (italic text next to each place, above the name of the place), and we omit all arc expressions, for readability reasons.

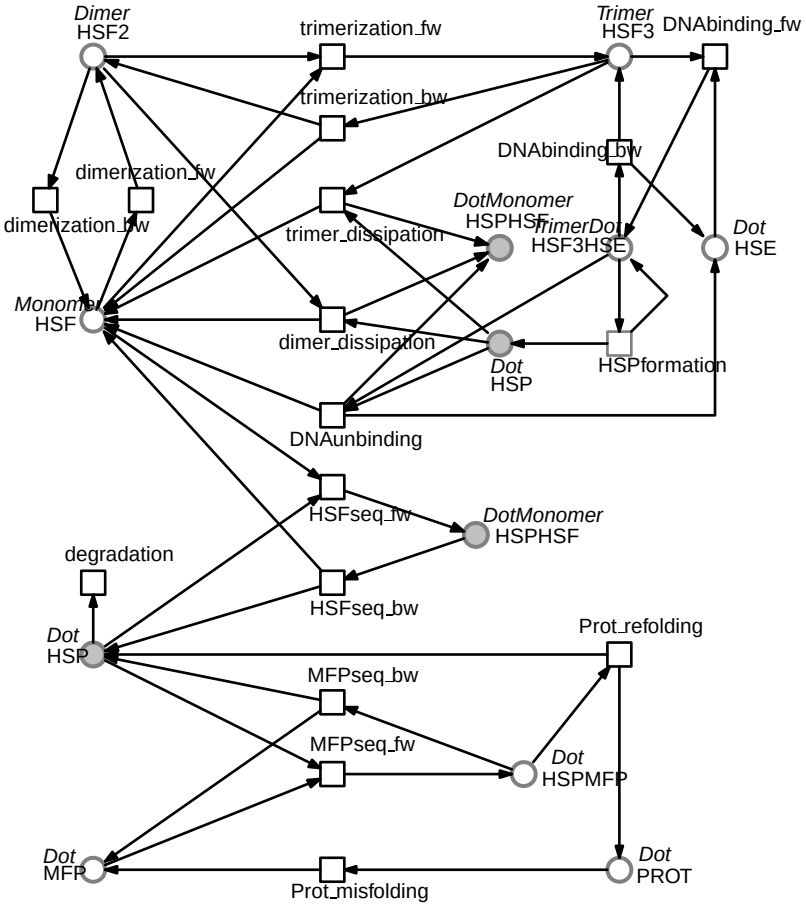

Figure 9: Snoopy representation of the color-focused refined heat shock response model. Some transitions are marked with variables, and the corresponding transitions have guards shown above as conditions of the form.

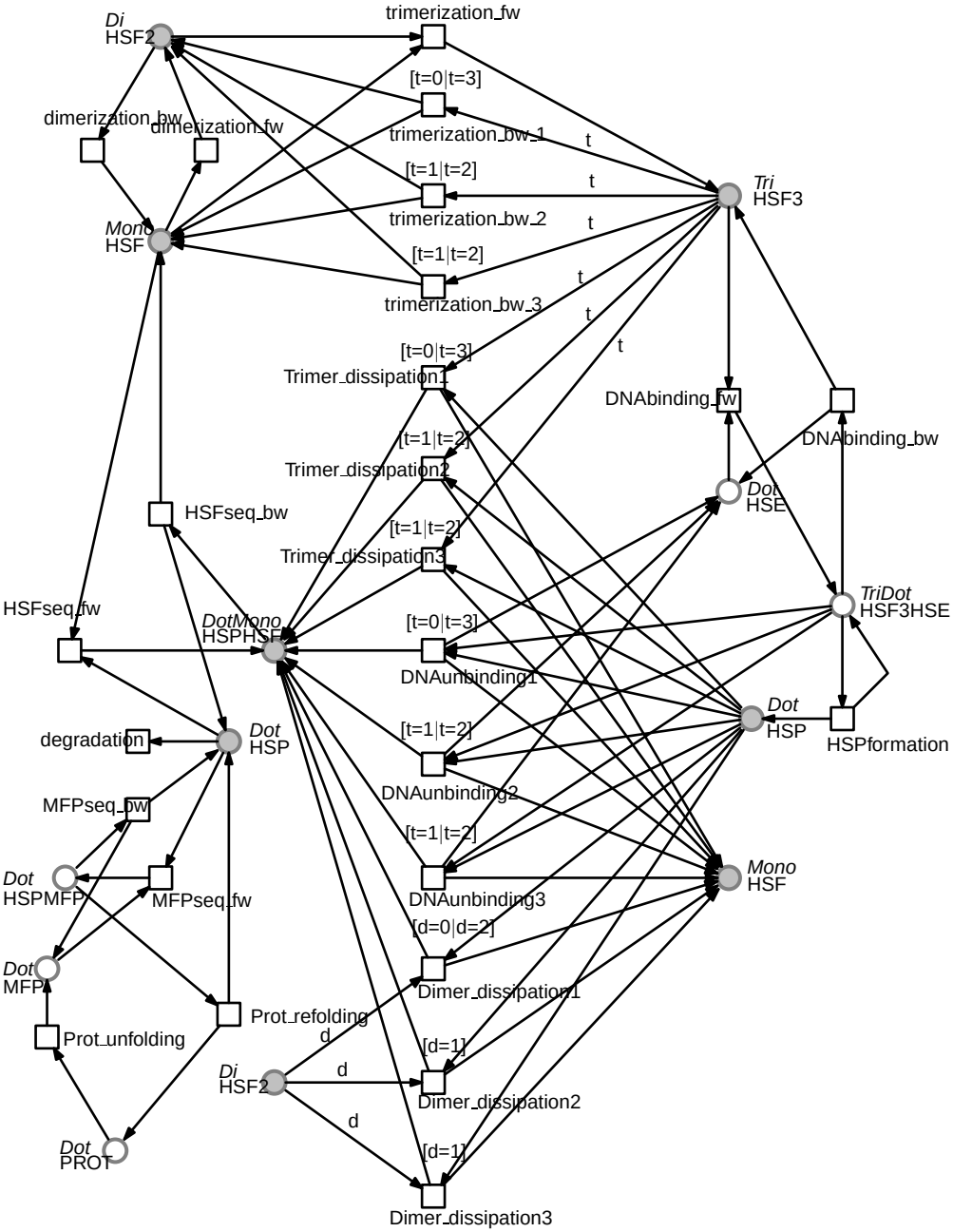

Table 9: The P-invariants for the basic eukaryotic heat shock response, as reported by the Charlie tool

No.	Components	Multiplicity
1	HSE	1
	HSF3HSE	1
2	HSF	1
	HSF2	2
	HSF3	3
	HSF3HSE	3
	HSPHSF	1
3	MFP	1
	HSPMFP	1
	PROT	1

Table 10: The T-invariants for the eukaryotic heat shock response, as reported by the Charlie tool

No.	Transition	No.	Transition
1	DNAbinding_bw	7	dimerization_fw
	DNAbinding_fw		trimerization_fw
2	trimerization_fw		HSFsequestration_bw
	trimerization_bw		DNAunbinding
3	dimerization_fw		DNAbinding_fw
	dimerization_bw	8	MFPsequestration_fw
4	HSFsequestration_bw		MFPsequestration_bw
	HSFsequestration_fw	9	MFPsequestration_fw
5	dimerization_fw		Protein_refolding
	HSFsequestration_bw		Protein_misfolding
	dimer_dissipation	10	degradation
6	dimerization_fw		HSPformation
	trimerization_fw		
	HSFsequestration_bw		
	trimer_dissipation		

D The PRISM implementation of the heat shock response models

Table 11: The PRISM implementation of the basic heat shock response model

ctmc

const int $N = 150000000$;
const int $N_{HSF} = 1602$;
const int $N_{HSF_2} = 1602/2$;
const int $N_{HSF_3} = 1602/3$;
const int $N_{HSE} = 30$;
const int $N_{PROT} = 10^8$;
const double $k_1 = 2 * 3.49$;
const double $k_2 = 0.19$;
const double $k_3 = 1.07$;
const double $k_4 = 1e-9$;
const double $k_5 = 0.17$;
const double $k_6 = 1.21e-6$;
const double $k_7 = 8.3e-3$;
const double $k_8 = 9.74$;
const double $k_9 = 3.56$;
const double $k_{10} = 2.33,$
const double $k_{11} = 4.31e-5$;
const double $k_{12} = 2.73e-7$;
const double $k_{13} = 3.2e-5$;
const double $k_{14} = 8.7e-06$;
const double $k_{15} = 3.32e-3$;
const double $k_{16} = 4.44$;
const double $k_{17} = 13.94$;

hsf: $[0..N_{HSF}]$ init 1;
hsf_2: $[0..N_{HSF_2}]$ init 0;
hsf_3: $[0..N_{HSF_3}]$ init 0;
hse: $[0..N_{HSE}]$ init 30;
hsf_3: hse: $[0..N_{HSE}]$ init 3;
hsp: $[0..N]$ init 766;
hsp: hsf: $[0..N_{HSF}]$ init 1403;
mfp: $[0..N_{PROT}]$ init 517;
hsp: mfp: $[0..N_{PROT}]$ init 71;
prot: $[0..N_{PROT}]$ init 114915000;

[formdimer] $\mathsf{hsf} >= 2$
$\wedge\, \mathsf{hsf}_2 <= N_{HSF_2} - 1$
$\rightarrow \mathsf{hsf} * (\mathsf{hsf} - 1) * 0.5 * k_1 :$
$(\mathsf{hsf}' = \mathsf{hsf} - 2) \wedge$
$(\mathsf{hsf}_2{}' = \mathsf{hsf}_2 + 1)$;

[decdimer] $\mathsf{hsf}_2 >= 1$
$\wedge\, \mathsf{hsf} <= N_{HSF} - 2$
$\rightarrow \mathsf{hsf}_2 * k_2 :$
$(\mathsf{hsf}_2{}' = \mathsf{hsf}_2 - 1)$
$\wedge (\mathsf{hsf}' = \mathsf{hsf} + 2)$;

[formtrimer] $\mathsf{hsf} >= 1$
$\wedge\, \mathsf{hsf}_2 >= 1$
$\wedge\, \mathsf{hsf}_3 <= N_{HSF_3} - 1$

[dectrimer] $\mathsf{hsf}_3 >= 1$
$\wedge\, \mathsf{hsf}_2 <= N_{HSF_2} - 2$
$\wedge\, \mathsf{hsf} <= N_{HSF} - 1$
$\rightarrow \mathsf{hsf}_3 * k_4 :$
$(\mathsf{hsf}_3{}' = \mathsf{hsf}_3 - 1)$
$\wedge (\mathsf{hsf}_2{}' = \mathsf{hsf}_2 + 1)$
$\wedge (\mathsf{hsf}' = \mathsf{hsf} + 1)$;

[dnabinding] $\mathsf{hsf}_3 >= 1$
$\wedge\, \mathsf{hse} >= 1 \wedge \mathsf{hsf}_3 \text{: hse} <= N_{HSE} - 1$
$\rightarrow \mathsf{hsf}_3 * \mathsf{hse} * k_5 :$
$(\mathsf{hsf}_3{}' = \mathsf{hsf}_3 - 1)$
$\wedge (\mathsf{hse}' = \mathsf{hse} - 1)$
$\wedge (\mathsf{hsf}_3 \text{: hse}' = \mathsf{hsf}_3 \text{: hse} + 1)$;

Table 11: The PRISM implementation of the basic heat shock response model - Continued

$\rightarrow \mathsf{hsf} * \mathsf{hsf_2} * k_3 :$
$(\mathsf{hsf_2}' = \mathsf{hsf_2} - 1)$
$\wedge (\mathsf{hsf}' = \mathsf{hsf} - 1)$
$\wedge (\mathsf{hsf_3}' = \mathsf{hsf_3} + 1);$

[hsfhsp] $\mathsf{hsp} >= 1$
$\wedge\, \mathsf{hsf} >= 1$
$\wedge\, \mathsf{hsp{:}\ hsf} <= N_{HSF} - 1$
$\rightarrow \mathsf{hsp} * \mathsf{hsf} * k_8 :$
$(\mathsf{hsp}' = \mathsf{hsp} - 1)$
$\wedge (\mathsf{hsf}' = \mathsf{hsf} - 1)$
$\wedge (\mathsf{hsp{:}\ hsf}' = \mathsf{hsp{:}\ hsf} + 1);$

[dimerhsp] $\mathsf{hsf_2} >= 1$
$\wedge\, \mathsf{hsp} >= 1$
$\wedge\, \mathsf{hsp{:}\ hsf} <= N_{HSF} - 1$
$\wedge\, \mathsf{hsf} <= N_{HSF} - 1$
$\rightarrow \mathsf{hsf_2} * \mathsf{hsp} * k_{10} :$
$(\mathsf{hsf_2}' = \mathsf{hsf_2} - 1)$
$\wedge (\mathsf{hsp}' = \mathsf{hsp} - 1)$
$\wedge (\mathsf{hsp{:}\ hsf}' = \mathsf{hsp{:}\ hsf} + 1)$
$\wedge (\mathsf{hsf}' = \mathsf{hsf} + 1);$

[misfolding] $\mathsf{prot} >= 1$
$\wedge\, \mathsf{mfp} <= N_{PROT} - 1$
$\rightarrow \mathsf{prot} * k_{14} :$
$(\mathsf{prot}' = \mathsf{prot} - 1)$
$\wedge (\mathsf{mfp}' = \mathsf{mfp} + 1);$

[hspdegrade] $\mathsf{hsp} >= 1$
$\rightarrow \mathsf{hsp} * k_{13} :$
$(\mathsf{hsp}' = \mathsf{hsp} - 1);$

[hspmfp] $\mathsf{hsp} >= 1$
$\wedge\, \mathsf{mfp} >= 1$
$\wedge\, \mathsf{hsp{:}\ mfp} <= N_{PROT} - 1$
$\rightarrow \mathsf{hsp} * \mathsf{mfp} * k_{15} :$
$(\mathsf{hsp}' = \mathsf{hsp} - 1)$
$\wedge (\mathsf{mfp}' = \mathsf{mfp} - 1)$
$\wedge (\mathsf{hsp{:}\ mfp}' = \mathsf{hsp{:}\ mfp} + 1);$

[dectrimerhse] $\mathsf{hsf_3{:}\ hse} >= 1$
$\wedge\, \mathsf{hsf_3} <= N_{HSF_3} - 1$
$\rightarrow \mathsf{hsf_3{:}\ hse} * k_6 : (\mathsf{hsf_3}' = \mathsf{hsf_3} + 1)$
$\wedge (\mathsf{hse}' = \mathsf{hse} + 1) \wedge (\mathsf{hsf_3{:}\ hse}' = \mathsf{hsf_3{:}\ hse} - 1);$

[trimerhsp] $\mathsf{hsf_3} >= 1$
$\wedge\, \mathsf{hsp} >= 1$
$\wedge\, \mathsf{hsp{:}\ hsf} <= N_{HSF} - 1$
$\wedge\, \mathsf{hsf} <= N_{HSF} - 2$
$\rightarrow \mathsf{hsf_3{:}\ hse} * \mathsf{hsp} * k_{11} :$
$(\mathsf{hsf_3}' = \mathsf{hsf_3} - 1)$
$\wedge (\mathsf{hsp}' = \mathsf{hsp} - 1)$
$\wedge (\mathsf{hsp{:}\ hsf}' = \mathsf{hsp{:}\ hsf} + 1)$
$\wedge (\mathsf{hsf}' = \mathsf{hsf} + 2);$

[decgene] $\mathsf{hsp} >= 1$
$\wedge\, \mathsf{hsf_3{:}\ hse} >= 1$
$\wedge\, \mathsf{hsp{:}\ hsf} <= N_{HSF} - 1$
$\wedge\, \mathsf{hse} <= N_{HSE} - 1$
$\wedge\, \mathsf{hsf} <= N_{HSF} - 2$
$\rightarrow \mathsf{hsp} * \mathsf{hsf_3{:}\ hse} * k_{12} :$
$(\mathsf{hsp}' = \mathsf{hsp} - 1)$
$\wedge (\mathsf{hsf_3{:}\ hse}' = \mathsf{hsf_3{:}\ hse} - 1)$
$\wedge (\mathsf{hsp{:}\ hsf}' = \mathsf{hsp{:}\ hsf} + 1)$
$\wedge (\mathsf{hse}' = \mathsf{hse} + 1)$
$\wedge (\mathsf{hsf}' = \mathsf{hsf} + 2);$

[formprot] $\mathsf{hsp{:}\ mfp} >= 1$

$\wedge\, \mathsf{hsp} <= N - 1$
$\wedge\, \mathsf{prot} <= N_{PROT} - 1$
$\rightarrow \mathsf{hsp{:}\ mfp} * k_{17} :$
$(\mathsf{hsp{:}\ mfp}' = \mathsf{hsp{:}\ mfp} - 1)$
$\wedge (\mathsf{hsp}' = \mathsf{hsp} + 1)$
$\wedge (\mathsf{prot}' = \mathsf{prot} + 1);$

Table 11: The PRISM implementation of the basic heat shock response model - Continued

[dechspmfp] $\mathsf{hsp}: \mathsf{mfp} >= 1$
$\wedge\, \mathsf{hsp} <= N - 1$
$\wedge\, \mathsf{mfp} <= N_{PROT} - 1 \rightarrow$
$\mathsf{hsp}: \mathsf{mfp} * k_{16}$:
$(\mathsf{hsp}: \mathsf{mfp}' = \mathsf{hsp}: \mathsf{mfp} - 1)$
$\wedge(\mathsf{hsp}' = \mathsf{hsp} + 1)$
$\wedge(\mathsf{mfp}' = \mathsf{mfp} + 1)$;

endmodule

Table 12: The PRISM implementation of the refined heat shock response model

ctmc

const int $N = 150000000$;
const int $N_{HSF} = 1602$;
const int $N_{HSF_2} = 1602/2$;
const int $N_{HSF_3} = 1602/3$;
const int $N_{HSE} = 30$;
const int $N_{PROT} = 10^8$;
const double $k_1 = 2 * 3.49$;
const double $k_2 = 0.19$;
const double $k_3 = 1.07$;
const double $k_4 = 1e-9$;
const double $k_5 = 0.17$;
const double $k_6 = 1.21e-6$;
const double $k_7 = 8.3e-3$;
const double $k_8 = 9.74$;
const double $k_9 = 3.56$;
const double $k_{10} = 2.33$,
const double $k_{11} = 4.31e-5$;
const double $k_{12} = 2.73e-7$;
const double $k_{13} = 3.2e-5$;
const double $k_{14} = 8.7e-06$;
const double $k_{15} = 3.32e-3$;
const double $k_{16} = 4.44$;
const double $k_{17} = 13.94$;

$\mathsf{rhsf} : [0..N_{HSF}]$ init 1;
$\mathsf{rhsf}^{(1)} : [0..N_{HSF}]$ init 0;
$\mathsf{rhsf_2} : [0..N_{HSF_2}]$ init 0;
$\mathsf{rhsf_2}^{(1)} : [0..N_{HSF_2}]$ init 0;
$\mathsf{rhsf_2}^{(2)} : [0..N_{HSF_2}]$ init 0;
$\mathsf{rhsf_3} : [0..N_{HSF_3}]$ init 0;
$\mathsf{rhsf_3}^{(1)} : [0..N_{HSF_3}]$ init 0;
$\mathsf{rhsf_3}^{(2)} : [0..N_{HSF_3}]$ init 0;
$\mathsf{rhsf_3}^{(3)} : [0..N_{HSF_3}]$ init 0;
$\mathsf{rhse} : [0..N_{HSE}]$ init 30;
$\mathsf{rhsf_3}$: $\mathsf{rhse} : [0..N_{HSE}]$ init 1;
$\mathsf{rhsf_3}$: $\mathsf{rhse}^{(1)} : [0..N_{HSE}]$ init 1;
$\mathsf{rhsf_3}$: $\mathsf{rhse}^{(2)} : [0..N_{HSE}]$ init 1;
$\mathsf{rhsf_3}$: $\mathsf{rhse}^{(3)} : [0..N_{HSE}]$ init 0;
$\mathsf{rhsp} : [0..N]$ init 766;
hsp: $\mathsf{rhsf} : [0..N_{HSF}]$ init 1309;
hsp: $\mathsf{rhsf}^{(1)} : [0..N_{HSF}]$ init 95;
$\mathsf{rmfp} : [0..N_{PROT}]$ init 517;
rhsp: $\mathsf{rmfp} : [0..N_{PROT}]$ init 71;
$\mathsf{rprot} : [0..N_{PROT}]$ init 114915000;

//Dimerization
$[]\ \mathsf{rhsf} >= 2 \wedge$
$\mathsf{rhsf_2} <= N_{HSF_2} - 1$
$\rightarrow \mathsf{rhsf} * \mathsf{rhsf} * 0.5 * k_1 :$
$(\mathsf{rhsf}' = \mathsf{rhsf} - 2)$
$\wedge(\mathsf{rhsf_2}' = \mathsf{rhsf_2} + 1);$

$[]\ \mathsf{rhsf} >= 1 \wedge \mathsf{rhsf}^{(1)} >= 1$
$\wedge\ \mathsf{rhsf_2}^{(1)} <= N_{HSF_2} - 1$
$\rightarrow \mathsf{rhsf} * \mathsf{rhsf}^{(1)} * k_1 :$
$(\mathsf{rhsf}' = \mathsf{rhsf} - 1)$
$\wedge(\mathsf{rhsf}^{(1)'} = \mathsf{rhsf}^{(1)} - 1)$
$\wedge(\mathsf{rhsf_2}^{(1)'} = \mathsf{rhsf_2}^{(1)} + 1);$

//Trimerization
$[]\ \mathsf{rhsf} >= 1 \wedge \mathsf{rhsf_2} >= 1$
$\wedge\ \mathsf{rhsf_3} <= N_{HSF_3} - 1$
$\rightarrow \mathsf{rhsf} * \mathsf{rhsf_2} * k_3 :$
$(\mathsf{rhsf_2}' = \mathsf{rhsf_2} - 1)$
$\wedge(\mathsf{rhsf}' = \mathsf{rhsf} - 1)$
$\wedge(\mathsf{rhsf_3}' = \mathsf{rhsf_3} + 1);$

$[]\ \mathsf{rhsf}^{(1)} >= 1 \wedge \mathsf{rhsf_2} >= 1$
$\wedge\ \mathsf{rhsf_3}^{(1)} <= N_{HSF_3} - 1$
$\rightarrow \mathsf{rhsf}^{(1)} * \mathsf{rhsf_2} * k_3 :$
$(\mathsf{rhsf_2}' = \mathsf{rhsf_2} - 1)$
$\wedge(\mathsf{rhsf}^{(1)'} = \mathsf{rhsf}^{(1)} - 1)$

Table 12: The PRISM implementation of the refined heat shock response model - Continued

$[]\ \mathsf{rhsf}^{(1)} >= 2 \wedge$
$\mathsf{rhsf_2}^{(2)} <= N_{HSF_2} - 1$
$\rightarrow\ \mathsf{rhsf}^{(1)} * (\mathsf{rhsf}^{(1)} - 1) * 0.5 * k_1 :$
$(\mathsf{rhsf}^{(1)'} = \mathsf{rhsf}^{(1)} - 2) \wedge$
$(\mathsf{rhsf_2}^{(2)'} = \mathsf{rhsf_2}^{(2)} + 1);$

//Reversed dimerization
$[]\ \mathsf{rhsf_2} >= 1 \wedge$
$\mathsf{rhsf} <= N_{HSF} - 2 \rightarrow \mathsf{rhsf_2} * k_2 :$
$(\mathsf{rhsf_2}' = \mathsf{rhsf_2} - 1)$
$\wedge (\mathsf{rhsf}' = \mathsf{rhsf} + 2);$

$[]\ \mathsf{rhsf_2}^{(1)} >= 1$
$\wedge\ \mathsf{rhsf} <= N_{HSF} - 1$
$\wedge\ \mathsf{rhsf}^{(1)} <= N_{HSF} - 1$
$\rightarrow\ \mathsf{rhsf_2}^{(1)} * k_2 :$
$(\mathsf{rhsf_2}^{(1)'} = \mathsf{rhsf_2}^{(1)} - 1)$
$\wedge (\mathsf{rhsf}' = \mathsf{rhsf} + 1)$
$\wedge (\mathsf{rhsf}^{(1)'} = \mathsf{rhsf}^{(1)} + 1);$

$[]\ \mathsf{rhsf_2}^{(2)} >= 1$
$\wedge\ \mathsf{rhsf}^{(1)} <= N_{HSF} - 2$
$\rightarrow\ \mathsf{rhsf_2}^{(2)} * k_2 :$
$(\mathsf{rhsf_2}^{(2)'} = \mathsf{rhsf_2}^{(2)} - 1)$
$\wedge (\mathsf{rhsf}^{(1)'} = \mathsf{rhsf}^{(1)} + 2);$

//Reversed trimerization
$[]\ \mathsf{rhsf_3} >= 1$
$\wedge\ \mathsf{rhsf_2} <= N_{HSF_2} - 1$
$\wedge\ \mathsf{rhsf} <= N_{HSF} - 1$
$\rightarrow\ \mathsf{rhsf_3} * k_4 :$
$(\mathsf{rhsf_3}' = \mathsf{rhsf_3} - 1)$
$\wedge (\mathsf{rhsf_2}' = \mathsf{rhsf_2} + 1)$
$\wedge (\mathsf{rhsf}' = \mathsf{rhsf} + 1);$
$[]\ \mathsf{rhsf_3}^{(1)} >= 1$
$\wedge\ \mathsf{rhsf_2} <= N_{HSF_2} - 1$
$\wedge\ \mathsf{rhsf}^{(1)} <= N_{HSF} - 1$
$\wedge (\mathsf{rhsf_3}^{(1)'} = \mathsf{rhsf_3}^{(1)} + 1);$

$[]\ \mathsf{rhsf} >= 1 \wedge \mathsf{rhsf_2}^{(1)} >= 1$
$\wedge\ \mathsf{rhsf_3}^{(1)} <= N_{HSF_3} - 1$
$\rightarrow\ \mathsf{rhsf} * \mathsf{rhsf_2}^{(1)} * k_3 :$
$(\mathsf{rhsf_2}^{(1)'} = \mathsf{rhsf_2}^{(1)} - 1)$
$\wedge (\mathsf{rhsf}' = \mathsf{rhsf} - 1)$
$\wedge (\mathsf{rhsf_3}^{(1)'} = \mathsf{rhsf_3}^{(1)} + 1);$

$[]\ \mathsf{rhsf}^{(1)} >= 1 \wedge \mathsf{rhsf_2}^{(1)} >= 1$
$\wedge\ \mathsf{rhsf_3}^{(2)} <= N_{HSF_3} - 1$
$\rightarrow\ \mathsf{rhsf}^{(1)} * \mathsf{rhsf_2}^{(1)} * k_3 :$
$(\mathsf{rhsf_2}^{(1)'} = \mathsf{rhsf_2}^{(1)} - 1)$
$\wedge (\mathsf{rhsf}^{(1)'} = \mathsf{rhsf}^{(1)} - 1)$
$\wedge (\mathsf{rhsf_3}^{(2)'} = \mathsf{rhsf_3}^{(2)} + 1);$

$[]\ \mathsf{rhsf} >= 1 \wedge \mathsf{rhsf_2}^{(2)} >= 1$
$\wedge\ \mathsf{rhsf_3}^{(2)} <= N_{HSF_3} - 1$
$\rightarrow\ \mathsf{rhsf} * \mathsf{rhsf_2}^{(2)} * k_3 :$
$(\mathsf{rhsf_2}^{(2)'} = \mathsf{rhsf_2}^{(2)} - 1)$
$\wedge (\mathsf{rhsf}' = \mathsf{rhsf} - 1)$
$\wedge (\mathsf{rhsf_3}^{(2)'} = \mathsf{rhsf_3}^{(2)} + 1);$
$[]\ \mathsf{rhsf}^{(1)} >= 1 \wedge \mathsf{rhsf_2}^{(2)} >= 1$
$\wedge\ \mathsf{rhsf_3}^{(3)} <= N_{HSF_3} - 1$
$\rightarrow\ \mathsf{rhsf}^{(1)} * \mathsf{rhsf_2}^{(2)} * k_3 :$

$(\mathsf{rhsf_2}^{(2)'} = \mathsf{rhsf_2}^{(2)} - 1)$
$\wedge (\mathsf{rhsf}^{(1)'} = \mathsf{rhsf}^{(1)} - 1)$
$\wedge (\mathsf{rhsf_3}^{(3)'} = \mathsf{rhsf_3}^{(3)} + 1);$

//Dna binding
$[]\ \mathsf{rhsf_3} >= 1 \wedge \mathsf{rhse} >= 1$
$\wedge\ \mathsf{rhsf_3{:}\,rhse} <= N_{HSE} - 1$
$\rightarrow\ \mathsf{rhsf_3} * \mathsf{rhse} * k_5 :$
$(\mathsf{rhsf_3}' = \mathsf{rhsf_3} - 1)$
$\wedge (\mathsf{rhse}' = \mathsf{rhse} - 1) \wedge$
$(\mathsf{rhsf_3{:}\,rhse}' = \mathsf{rhsf_3{:}\,rhse} + 1)$

Table 12: The PRISM implementation of the refined heat shock response model - Continued

$\rightarrow \mathsf{rhsf_3}^{(1)} * k_4$:
$(\mathsf{rhsf_3}^{(1)'} = \mathsf{rhsf_3}^{(1)} - 1)$
$\wedge (\mathsf{rhsf_2}' = \mathsf{rhsf_2} + 1)$
$\wedge (\mathsf{rhsf}^{(1)'} = \mathsf{rhsf}^{(1)} + 1)$;

$[]\ \mathsf{rhsf_3}^{(1)} >= 1$
$\wedge\, \mathsf{rhsf_2}^{(1)} <= N_{HSF_2} - 1$
$\wedge\, \mathsf{rhsf} <= N_{HSF} - 1$
$\rightarrow \mathsf{rhsf_3}^{(1)} * k_4$:
$(\mathsf{rhsf_3}^{(1)'} = \mathsf{rhsf_3}^{(1)} - 1)$
$\wedge (\mathsf{rhsf_2}^{(1)'} = \mathsf{rhsf_2}^{(1)} + 1)$
$\wedge (\mathsf{rhsf}' = \mathsf{rhsf} + 1)$;

$[]\ \mathsf{rhsf_3}^{(2)} >= 1$
$\wedge\, \mathsf{rhsf_2}^{(1)} <= N_{HSF_2} - 1$
$\wedge\, \mathsf{rhsf}^{(1)} <= N_{HSF} - 1$
$\rightarrow \mathsf{rhsf_3}^{(2)} * k_4$:
$(\mathsf{rhsf_3}^{(2)'} = \mathsf{rhsf_3}^{(2)} - 1)$
$\wedge (\mathsf{rhsf_2}^{(1)'} = \mathsf{rhsf_2}^{(1)} + 1)$
$\wedge (\mathsf{rhsf}^{(1)'} = \mathsf{rhsf}^{(1)} + 1)$;

$[]\ \mathsf{rhsf_3}^{(2)} >= 1$
$\wedge\, \mathsf{rhsf_2}^{(2)} <= N_{HSF_2} - 1$
$\wedge\, \mathsf{rhsf} <= N_{HSF} - 1$
$\rightarrow \mathsf{rhsf_3}^{(2)} * k_4$:
$(\mathsf{rhsf_3}^{(2)'} = \mathsf{rhsf_3}^{(2)} - 1)$
$\wedge (\mathsf{rhsf_2}^{(2)'} = \mathsf{rhsf_2}^{(2)} + 1)$
$\wedge (\mathsf{rhsf}' = \mathsf{rhsf} + 1)$;

$[]\ \mathsf{rhsf_3}^{(3)} >= 1$
$\wedge\, \mathsf{rhsf_2}^{(2)} <= N_{HSF_2} - 1$
$\wedge\, \mathsf{rhsf}^{(1)} <= N_{HSF} - 1$
$\rightarrow \mathsf{rhsf_3}^{(3)} * k_4$:
$(\mathsf{rhsf_3}^{(3)'} =$
$\mathsf{rhsf_3}^{(3)} - 1)$
$\wedge (\mathsf{rhsf_2}^{(2)'} =$
$\mathsf{rhsf_2}^{(2)} + 1)$

$[]\ \mathsf{rhsf_3}^{(1)} >= 1 \wedge \mathsf{rhse} >= 1$
$\wedge\, \mathsf{rhsf_3}\colon \mathsf{rhse}^{(1)} <= N_{HSE} - 1$
$\rightarrow \mathsf{rhsf_3}^{(1)} * \mathsf{rhse} * k_5$:
$(\mathsf{rhsf_3}^{(1)'} =$
$\mathsf{rhsf_3}^{(1)} - 1)$
$\wedge (\mathsf{rhse}' = \mathsf{rhse} - 1) \wedge$
$(\mathsf{rhsf_3}\colon \mathsf{rhse}^{(1)'} =$
$\mathsf{rhsf_3}\colon \mathsf{rhse}^{(1)} + 1)$;

$[]\ \mathsf{rhsf_3}^{(2)} >= 1 \wedge \mathsf{rhse} >= 1$
$\wedge\, \mathsf{rhsf_3}\colon \mathsf{rhse}^{(2)} <= N_{HSE} - 1$
$\rightarrow \mathsf{rhsf_3}^{(2)} * \mathsf{rhse} * k_5$:
$(\mathsf{rhsf_3}^{(2)'} =$
$\mathsf{rhsf_3}^{(2)} - 1)$
$\wedge (\mathsf{rhse}' = \mathsf{rhse} - 1) \wedge$
$(\mathsf{rhsf_3}\colon \mathsf{rhse}^{(2)'} =$
$\mathsf{rhsf_3}\colon \mathsf{rhse}^{(2)} + 1)$;
$[]\ \mathsf{rhsf_3}^{(3)} >= 1 \wedge \mathsf{rhse} >= 1$
$\wedge\, \mathsf{rhsf_3}\colon \mathsf{rhse}^{(3)} <= N_{HSE} - 1$
$\rightarrow \mathsf{rhsf_3}^{(3)} * \mathsf{rhse} * k_5$:
$(\mathsf{rhsf_3}^{(3)'} =$
$\mathsf{rhsf_3}^{(3)} - 1)$
$\wedge (\mathsf{rhse}' = \mathsf{rhse} - 1) \wedge$
$(\mathsf{rhsf_3}\colon \mathsf{rhse}^{(3)} =$
$\mathsf{rhsf_3}\colon \mathsf{rhse}^{(3)} + 1)$;

//Reversed dna binding
$[]\ \mathsf{rhsf_3}\colon \mathsf{rhse} >= 1$

$\wedge\, \mathsf{rhse} <= N_{HSE} - 1$
$\wedge\, \mathsf{rhsf_3} <= N_{HSF_3} - 1$
$\rightarrow \mathsf{rhsf_3}\colon \mathsf{rhse} * k_6$:
$(\mathsf{rhsf_3}' = \mathsf{rhsf_3} + 1)$
$\wedge (\mathsf{rhse}' = \mathsf{rhse} + 1)$
$\wedge (\mathsf{rhsf_3}\colon \mathsf{rhse}' = \mathsf{rhsf_3}\colon \mathsf{rhse} - 1)$;

$[]\ \mathsf{rhsf_3}\colon \mathsf{rhse}^{(1)} >= 1$

Table 12: The PRISM implementation of the refined heat shock response model - Continued

$\wedge(\mathsf{rhsf}^{(1)'} = \mathsf{rhsf}^{(1)} + 1);$

//HSP transcription

$[]\ \mathsf{rhsf_3}\colon \mathsf{rhse} >= 1$
$\wedge\, \mathsf{rhsp} <= N - 1$
$\rightarrow\ \mathsf{rhsf_3}\colon \mathsf{rhse} * k_7 :$
$(\mathsf{rhsp}' = \mathsf{rhsp} + 1);$

$[]\ \mathsf{rhsf_3}\colon \mathsf{rhse}^{(1)} >= 1$
$\wedge\, \mathsf{rhsp} <= N - 1$
$\rightarrow\ \mathsf{rhsf_3}\colon \mathsf{rhse}^{(1)} * k_7 :$
$(\mathsf{rhsp}' = \mathsf{rhsp} + 1)$

$[]\ \mathsf{rhsf_3}\colon \mathsf{rhse}^{(2)} >= 1$
$\wedge\, \mathsf{rhsp} <= N - 1$
$\rightarrow\ \mathsf{rhsf_3}\colon \mathsf{rhse}^{(2)} * k_7 :$
$(\mathsf{rhsp}' = \mathsf{rhsp} + 1);$

//Sequestration of HSF

by HSP

$[]\ \mathsf{rhsf_3}\colon \mathsf{rhse}^{(3)} >= 1$
$\wedge\, \mathsf{rhsp} <= N - 1$
$\rightarrow\ \mathsf{rhsf_3}\colon \mathsf{rhse}^{(3)} * k_7 :$
$(\mathsf{rhsp}' = \mathsf{rhsp} + 1);$

$[]\ \mathsf{rhsp} >= 1 \wedge \mathsf{rhsf} >= 1$
$\wedge\, \mathsf{hsp}\colon \mathsf{rhsf} <= N_{HSF} - 1$
$\rightarrow\ \mathsf{rhsp} * \mathsf{rhsf} * k_8 :$
$(\mathsf{rhsp}' = \mathsf{rhsp} - 1)$
$\wedge(\mathsf{rhsf}' = \mathsf{rhsf} - 1)$
$\wedge(\mathsf{hsp}\colon \mathsf{rhsf}' = \mathsf{hsp}\colon \mathsf{rhsf} + 1);$

$[]\ \mathsf{rhsp} >= 1 \wedge \mathsf{rhsf}^{(1)} >= 1$
$\wedge\, \mathsf{hsp}\colon \mathsf{rhsf}^{(1)} <= N_{HSF} - 1$
$\rightarrow\ \mathsf{rhsp} * \mathsf{rhsf} * k_8 :$
$(\mathsf{rhsp}' = \mathsf{rhsp} - 1)$
$\wedge\, \mathsf{rhse} <= N_{HSE} - 1$
$\wedge\, \mathsf{rhsf_3}^{(1)} <= N_{HSF_3} - 1$
$\rightarrow\ \mathsf{rhsf_3}\colon \mathsf{rhse}^{(1)} * k_6 :$
$(\mathsf{rhsf_3}^{(1)'} =$
$\mathsf{rhsf_3}^{(1)} + 1)$
$\wedge(\mathsf{rhse}' = \mathsf{rhse} + 1)\wedge$
$(\mathsf{rhsf_3}\colon \mathsf{rhse}^{(1)'} = \mathsf{rhsf_3}\colon \mathsf{rhse}^{(1)} - 1);$

$[]\ \mathsf{rhsf_3}\colon \mathsf{rhse}^{(2)} >= 1$
$\wedge\, \mathsf{rhse} <= N_{HSE} - 1$
$\wedge\, \mathsf{rhsf_3}^{(2)} <= N_{HSF_3} - 1$
$\rightarrow\ \mathsf{rhsf_3}\colon \mathsf{rhse}^{(2)} * k_6 :$
$(\mathsf{rhsf_3}^{(2)'} = \mathsf{rhsf_3}^{(2)} + 1)$
$\wedge(\mathsf{rhse}' = \mathsf{rhse} + 1)\wedge$
$(\mathsf{rhsf_3}\colon \mathsf{rhse}^{(2)'} =$
$\mathsf{rhsf_3}\colon \mathsf{rhse}^{(2)} - 1);$

$[]\ \mathsf{rhsf_3}\colon \mathsf{rhse}^{(3)} >= 1$

$\wedge\, \mathsf{rhse} <= N_{HSE} - 1$

$\wedge\, \mathsf{rhsf_3}^{(3)} <= N_{HSF_3} - 1$
$\rightarrow\ \mathsf{rhsf_3}\colon \mathsf{rhse}^{(3)} * k_6 :$
$(\mathsf{rhsf_3}^{(3)'} = \mathsf{rhsf_3}^{(3)} + 1)$
$\wedge(\mathsf{rhse}' = \mathsf{rhse} + 1)\wedge$
$(\mathsf{rhsf_3}\colon \mathsf{rhse}^{(3)'} =$
$\mathsf{rhsf_3}\colon \mathsf{rhse}^{(3)} - 1);$

//hsp:hsf unbinding

$[]\ \mathsf{hsp}\colon \mathsf{rhsf} >= 1$
$\wedge\, \mathsf{rhsp} <= N - 1$
$\wedge\, \mathsf{rhsf} <= N_{HSF} - 1$
$\rightarrow\ \mathsf{hsp}\colon \mathsf{rhsf} * k_9 :$
$(\mathsf{hsp}\colon \mathsf{rhsf}' = \mathsf{hsp}\colon \mathsf{rhsf} - 1)$
$\wedge(\mathsf{rhsp}' = \mathsf{rhsp} + 1)$
$\wedge(\mathsf{rhsf}' = \mathsf{rhsf} + 1);$

$[]\ \mathsf{hsp}\colon \mathsf{rhsf}^{(1)} >= 1$

Table 12: The PRISM implementation of the refined heat shock response model - Continued

$\wedge(\mathsf{rhsf}^{(1)'} = \mathsf{rhsf}^{(1)} - 1)\wedge$
$(\mathsf{hsp}\colon \mathsf{rhsf}^{(1)'} = \mathsf{hsp}\colon \mathsf{rhsf}^{(1)} + 1);$

//Sequestration of dimer by HSP

$[]\ \mathsf{rhsf}_2 >= 1 \wedge \mathsf{rhsp} >= 1$
$\wedge\ \mathsf{hsp}\colon \mathsf{rhsf} <= N_{HSF} - 1$
$\wedge\ \mathsf{rhsf} <= N_{HSF} - 1$
$\rightarrow\ \mathsf{rhsf}_2 * \mathsf{rhsp} * k_{10}:$
$(\mathsf{rhsf}_2{}' = \mathsf{rhsf}_2 - 1)$
$\wedge(\mathsf{rhsp}' = \mathsf{rhsp} - 1)$
$\wedge(\mathsf{hsp}\colon \mathsf{rhsf}' = \mathsf{hsp}\colon \mathsf{rhsf} + 1)$
$\wedge(\mathsf{rhsf}' = \mathsf{rhsf} + 1);$

$[]\ \mathsf{rhsf}_2{}^{(1)} >= 1 \wedge \mathsf{rhsp} >= 1$
$\wedge\ \mathsf{hsp}\colon \mathsf{rhsf} <= N_{HSF} - 1$
$\wedge\ \mathsf{rhsf} <= N_{HSF} - 1$
$\rightarrow\ \mathsf{rhsf}_2{}^{(1)} * \mathsf{rhsp} * k_{10}:$
$(\mathsf{rhsf}_2{}^{(1)'} = \mathsf{rhsf}_2{}^{(1)} - 1)$
$\wedge(\mathsf{rhsp}' = \mathsf{rhsp} - 1)$
$\wedge(\mathsf{hsp}\colon \mathsf{rhsf}' = \mathsf{hsp}\colon \mathsf{rhsf} + 1)$
$\wedge(\mathsf{rhsf}^{(1)'} = \mathsf{rhsf}^{(1)} + 1);$

$[]\ \mathsf{rhsf}_2{}^{(1)} >= 1 \wedge \mathsf{rhsp} >= 1$
$\wedge\ \mathsf{hsp}\colon \mathsf{rhsf}^{(1)} <= N_{HSF} - 1$
$\wedge\ \mathsf{rhsf} <= N_{HSF} - 1$
$\rightarrow\ \mathsf{rhsf}_2{}^{(1)} * \mathsf{rhsp} * k_{10}:$
$(\mathsf{rhsf}_2{}^{(1)'} = \mathsf{rhsf}_2{}^{(1)} - 1)$
$\wedge(\mathsf{rhsp}' = \mathsf{rhsp} - 1)\wedge$
$(\mathsf{hsp}\colon \mathsf{rhsf}^{(1)'} = \mathsf{hsp}\colon \mathsf{rhsf}^{(1)} + 1)$
$\wedge(\mathsf{rhsf}' = \mathsf{rhsf} + 1);$

$[]\ \mathsf{rhsf}_2{}^{(2)} >= 1 \wedge \mathsf{rhsp} >= 1$
$\wedge\ \mathsf{hsp}\colon \mathsf{rhsf}^{(1)} <= N_{HSF} - 1$
$\wedge\ \mathsf{rhsf}^{(1)} <= N_{HSF} - 1$
$\rightarrow\ \mathsf{rhsf}_2{}^{(2)} * \mathsf{rhsp} * k_{10}:$
$(\mathsf{rhsf}_2{}^{(2)'} = \mathsf{rhsf}_2{}^{(2)} - 1)$
$\wedge(\mathsf{rhsp}' = \mathsf{rhsp} - 1)\wedge$
$\wedge\ \mathsf{rhsp} <= N - 1$
$\wedge\ \mathsf{rhsf}^{(1)} <= N_{HSF} - 1$
$\rightarrow\ \mathsf{hsp}\colon \mathsf{rhsf}^{(1)} * k_9:$
$(\mathsf{hsp}\colon \mathsf{rhsf}^{(1)'} = \mathsf{hsp}\colon \mathsf{rhsf}^{(1)} - 1)$
$\wedge(\mathsf{rhsp}' = \mathsf{rhsp} + 1)\wedge$
$(\mathsf{rhsf}^{(1)'} = \mathsf{rhsf}^{(1)} + 1);$

//Sequestration of trimer by HSP

$[]\ \mathsf{rhsf}_3 >= 1 \wedge \mathsf{rhsp} >= 1$
$\wedge\ \mathsf{hsp}\colon \mathsf{rhsf} <= N_{HSF} - 1$
$\wedge\ \mathsf{rhsf} <= N_{HSF} - 2$
$\rightarrow\ \mathsf{rhsf}_3 * \mathsf{rhsp} * k_{11}:$
$(\mathsf{rhsf}_3{}' = \mathsf{rhsf}_3 - 1)$
$\wedge(\mathsf{rhsp}' = \mathsf{rhsp} - 1)$
$\wedge(\mathsf{hsp}\colon \mathsf{rhsf}' = \mathsf{hsp}\colon \mathsf{rhsf} + 1)$
$\wedge(\mathsf{rhsf}' = \mathsf{rhsf} + 2);$

$[]\ \mathsf{rhsf}_3{}^{(1)} >= 1 \wedge \mathsf{rhsp} >= 1$
$\wedge\ \mathsf{hsp}\colon \mathsf{rhsf}^{(1)} <= N_{HSF} - 1$
$\wedge\ \mathsf{rhsf} <= N_{HSF} - 2$
$\rightarrow\ \mathsf{rhsf}_3{}^{(1)} * \mathsf{rhsp} * k_{11}:$
$(\mathsf{rhsf}_3{}^{(1)'} = \mathsf{rhsf}_3{}^{(1)} - 1)$
$\wedge(\mathsf{rhsp}' = \mathsf{rhsp} - 1)\wedge$
$(\mathsf{hsp}\colon \mathsf{rhsf}^{(1)'} = \mathsf{hsp}\colon \mathsf{rhsf}^{(1)} + 1)$
$\wedge(\mathsf{rhsf}' = \mathsf{rhsf} + 2);$

$[]\ \mathsf{rhsf}_3{}^{(1)} >= 1 \wedge \mathsf{rhsp} >= 1$
$\wedge\ \mathsf{hsp}\colon \mathsf{rhsf} <= N_{HSF} - 1$
$\wedge\ \mathsf{rhsf} <= N_{HSF} - 1$
$\wedge\ \mathsf{rhsf}^{(1)} <= N_{HSF} - 1$
$\rightarrow\ \mathsf{rhsf}_3{}^{(1)} * \mathsf{rhsp} * k_{11}:$
$(\mathsf{rhsf}_3{}^{(1)'} = \mathsf{rhsf}_3{}^{(1)} - 1)$
$\wedge(\mathsf{rhsp}' = \mathsf{rhsp} - 1)\wedge$
$(\mathsf{hsp}\colon \mathsf{rhsf}' = \mathsf{hsp}\colon \mathsf{rhsf} + 1)$
$\wedge(\mathsf{rhsf}' = \mathsf{rhsf} + 1)$
$\wedge(\mathsf{rhsf}^{(1)'} = \mathsf{rhsf}^{(1)} + 1);$
$[]\ \mathsf{rhsf}_3{}^{(2)} >= 1 \wedge \mathsf{rhsp} >= 1$

Table 12: The PRISM implementation of the refined heat shock response model - Continued

$(\mathsf{hsp}\colon \mathsf{rhsf}^{(1)'} = \mathsf{hsp}\colon \mathsf{rhsf}^{(1)} + 1)$
$\wedge(\mathsf{rhsf}^{(1)'} = \mathsf{rhsf}^{(1)} + 1);$

//Gene unbinding
$[]\ \mathsf{rhsp} >= 1 \wedge \mathsf{rhsf_3}\colon \mathsf{rhse} >= 1$
$\wedge\ \mathsf{hsp}\colon \mathsf{rhsf} <= N_{HSF} - 1$
$\wedge\ \mathsf{rhse} <= N_{HSE} - 1$
$\wedge\ \mathsf{rhsf} <= N_{HSF} - 2$
$\rightarrow\ \mathsf{rhsp} * \mathsf{rhsf_3}\colon \mathsf{rhse} * k_{12}\ :$
$(\mathsf{rhsp}' = \mathsf{rhsp} - 1)$
$\wedge(\mathsf{rhsf_3}\colon \mathsf{rhse}' = \mathsf{rhsf_3}\colon \mathsf{rhse} - 1)$
$\wedge(\mathsf{hsp}\colon \mathsf{rhsf}' = \mathsf{hsp}\colon \mathsf{rhsf} + 1)$
$\wedge(\mathsf{rhse}' = \mathsf{rhse} + 1)$
$\wedge(\mathsf{rhsf}' = \mathsf{rhsf} + 2);$

$[]\ \mathsf{rhsp} >= 1 \wedge \mathsf{rhsf_3}\colon \mathsf{rhse}^{(1)} >= 1$
$\wedge\ \mathsf{hsp}\colon \mathsf{rhsf}^{(1)} <= N_{HSF} - 1$
$\wedge\ \mathsf{rhse} <= N_{HSE} - 1$
$\wedge\ \mathsf{rhsf} <= N_{HSF} - 2$
$\rightarrow\ \mathsf{rhsp} * \mathsf{rhsf_3}\colon \mathsf{rhse}^{(1)} * k_{12}\ :$
$(\mathsf{rhsp}' = \mathsf{rhsp} - 1)\wedge$
$(\mathsf{rhsf_3}\colon \mathsf{rhse}^{(1)'} = \mathsf{rhsf_3}\colon \mathsf{rhse}^{(1)} - 1)$
$\wedge(\mathsf{hsp}\colon \mathsf{rhsf}^{(1)'} = \mathsf{hsp}\colon \mathsf{rhsf}^{(1)} + 1)$
$\wedge(\mathsf{rhse}' = \mathsf{rhse} + 1)$
$\wedge(\mathsf{rhsf}' = \mathsf{rhsf} + 2);$

$[]\ \mathsf{rhsp} >= 1 \wedge \mathsf{rhsf_3}\colon \mathsf{rhse}^{(1)} >= 1$
$\wedge\ \mathsf{hsp}\colon \mathsf{rhsf} <= N_{HSF} - 1$
$\wedge\ \mathsf{rhse} <= N_{HSE} - 1$
$\wedge\ \mathsf{rhsf} <= N_{HSF} - 1$
$\wedge\ \mathsf{rhsf}^{(1)} <= N_{HSF} - 1$
$\rightarrow\ \mathsf{rhsp} * \mathsf{rhsf_3}\colon \mathsf{rhse}^{(1)} * k_{12}\ :$
$(\mathsf{rhsp}' = \mathsf{rhsp} - 1)\wedge$
$(\mathsf{rhsf_3}\colon \mathsf{rhse}^{(1)'} = \mathsf{rhsf_3}\colon \mathsf{rhse}^{(1)} - 1)$
$\wedge(\mathsf{hsp}\colon \mathsf{rhsf}' = \mathsf{hsp}\colon \mathsf{rhsf} + 1)$
$\wedge(\mathsf{rhse}' = \mathsf{rhse} + 1)$
$\wedge(\mathsf{rhsf}' = \mathsf{rhsf} + 1)$
$\wedge(\mathsf{rhsf}^{(1)'} = \mathsf{rhsf}^{(1)} + 1);$

$\wedge\ \mathsf{hsp}\colon \mathsf{rhsf} <= N_{HSF} - 1$
$\wedge\ \mathsf{rhsf}^{(1)} <= N_{HSF} - 2$
$\rightarrow\ \mathsf{rhsf_3}^{(2)} * \mathsf{rhsp} * k_{11}\ :$
$(\mathsf{rhsf_3}^{(2)'} = \mathsf{rhsf_3}^{(2)} - 1)$
$\wedge(\mathsf{rhsp}' = \mathsf{rhsp} - 1)\wedge$
$(\mathsf{hsp}\colon \mathsf{rhsf}' = \mathsf{hsp}\colon \mathsf{rhsf} + 1)$
$\wedge(\mathsf{rhsf}^{(1)'} = \mathsf{rhsf}^{(1)} + 2);$
$[]\ \mathsf{rhsf_3}^{(2)} >= 1 \wedge \mathsf{rhsp} >= 1$
$\wedge\ \mathsf{hsp}\colon \mathsf{rhsf}^{(1)} <= N_{HSF} - 1$
$\wedge\ \mathsf{rhsf} <= N_{HSF} - 1$
$\wedge\ \mathsf{rhsf}^{(1)} <= N_{HSF} - 1$
$\rightarrow\ \mathsf{rhsf_3}^{(2)} * \mathsf{rhsp} * k_{11}\ :$
$(\mathsf{rhsf_3}^{(2)'} = \mathsf{rhsf_3}^{(2)} - 1)$
$\wedge(\mathsf{rhsp}' = \mathsf{rhsp} - 1)\wedge$
$(\mathsf{hsp}\colon \mathsf{rhsf}^{(1)'} = \mathsf{hsp}\colon \mathsf{rhsf}^{(1)} + 1)$
$\wedge(\mathsf{rhsf}^{(1)'} = \mathsf{rhsf}^{(1)} + 1)$
$\wedge(\mathsf{rhsf}' = \mathsf{rhsf} + 1);$

$[]\ \mathsf{rhsf_3}^{(3)} >= 1 \wedge \mathsf{rhsp} >= 1$
$\wedge\ \mathsf{hsp}\colon \mathsf{rhsf}^{(1)} <= N_{HSF} - 1$
$\wedge\ \mathsf{rhsf}^{(1)} <= N_{HSF} - 2$
$\rightarrow\ \mathsf{rhsf_3}^{(3)} * \mathsf{rhsp} * k_{11}\ :$
$(\mathsf{rhsf_3}^{(3)'} = \mathsf{rhsf_3}^{(3)} - 1)$
$\wedge(\mathsf{rhsp}' = \mathsf{rhsp} - 1)\wedge$
$(\mathsf{hsp}\colon \mathsf{rhsf}^{(1)'} = \mathsf{hsp}\colon \mathsf{rhsf}^{(1)} + 1)$
$\wedge(\mathsf{rhsf}^{(1)'} = \mathsf{rhsf}^{(1)} + 2);$

//HSP degradation
$[]\ \mathsf{rhsp} >= 1 \rightarrow \mathsf{rhsp} * k_{13}\ :$
$(\mathsf{rhsp}' = \mathsf{rhsp} - 1);$

//Misfolding protein
$[]\ \mathsf{rprot} >= 1$
$\wedge\ \mathsf{rmfp} <= N_{PROT} - 1$
$\rightarrow\ \mathsf{rprot} * k_{14}\ :$
$(\mathsf{rprot}' = \mathsf{rprot} - 1)$
$\wedge(\mathsf{rmfp}' = \mathsf{rmfp} + 1);$

Table 12: The PRISM implementation of the refined heat shock response model - Continued

$[]\ \mathsf{rhsp} >= 1 \wedge \mathsf{rhsf_3{:}\,rhse}^{(2)} >= 1$
$\wedge\, \mathsf{hsp{:}\,rhsf}^{(1)} <= N_{HSF} - 1$
$\wedge\, \mathsf{rhse} <= N_{HSE} - 1$
$\wedge\, \mathsf{rhsf} <= N_{HSF} - 1$
$\wedge\, \mathsf{rhsf}^{(1)} <= N_{HSF} - 1$
$\rightarrow \mathsf{rhsp} * \mathsf{rhsf_3{:}\,rhse}^{(2)} * k_{12}$:
$(\mathsf{rhsp}' = \mathsf{rhsp} - 1) \wedge$
$(\mathsf{rhsf_3{:}\,rhse}^{(2)'} = \mathsf{rhsf_3{:}\,rhse}^{(2)} - 1)$
$\wedge(\mathsf{hsp{:}\,rhsf}^{(1)'} = \mathsf{hsp{:}\,rhsf}^{(1)} + 1)$
$\wedge(\mathsf{rhse}' = \mathsf{rhse} + 1)$
$\wedge(\mathsf{rhsf}' = \mathsf{rhsf} + 1)$
$\wedge(\mathsf{rhsf}^{(1)'} = \mathsf{rhsf}^{(1)} + 1);$

$[]\ \mathsf{rhsp} >= 1 \wedge \mathsf{rhsf_3{:}\,rhse}^{(2)} >= 1$
$\wedge\, \mathsf{hsp{:}\,rhsf} <= N_{HSF} - 1$
$\wedge\, \mathsf{rhse} <= N_{HSE} - 1$
$\wedge\, \mathsf{rhsf}^{(1)} <= N_{HSF} - 2$
$\rightarrow \mathsf{rhsp} * \mathsf{rhsf_3{:}\,rhse}^{(2)} * k_{12}$:
$(\mathsf{rhsp}' = \mathsf{rhsp} - 1) \wedge$
$(\mathsf{rhsf_3{:}\,rhse}^{(2)'} = \mathsf{rhsf_3{:}\,rhse}^{(2)} - 1)$
$\wedge(\mathsf{hsp{:}\,rhsf}' = \mathsf{hsp{:}\,rhsf} + 1)$
$\wedge(\mathsf{rhse}' = \mathsf{rhse} + 1)$
$\wedge(\mathsf{rhsf}^{(1)'} = \mathsf{rhsf}^{(1)} + 2);$

$[]\ \mathsf{rhsp} >= 1 \wedge \mathsf{rhsf_3{:}\,rhse}^{(3)} >= 1$
$\wedge\, \mathsf{hsp{:}\,rhsf}^{(1)} <= N_{HSF} - 1$
$\wedge\, \mathsf{rhse} <= N_{HSE} - 1$
$\wedge\, \mathsf{rhsf}^{(1)} <= N_{HSF} - 2$
$\rightarrow \mathsf{rhsp} * \mathsf{rhsf_3{:}\,rhse}^{(3)} * k_{12}$:
$(\mathsf{rhsp}' = \mathsf{rhsp} - 1) \wedge$
$(\mathsf{rhsf_3{:}\,rhse}^{(3)'} = \mathsf{rhsf_3{:}\,rhse}^{(3)} - 1)$
$\wedge(\mathsf{hsp{:}\,rhsf}^{(1)'} = \mathsf{hsp{:}\,rhsf}^{(1)} + 1)$
$\wedge(\mathsf{rhse}' = \mathsf{rhse} + 1)$

$\wedge(\mathsf{rhsf}^{(1)'} = \mathsf{rhsf}^{(1)} + 2);$

endmodule

//HSP and MFP binding
$[]\ \mathsf{rhsp} >= 1 \wedge \mathsf{rmfp} >= 1$
$\wedge\, \mathsf{rhsp{:}\,rmfp} <= N_{PROT} - 1$
$\rightarrow \mathsf{rhsp} * \mathsf{rmfp} * k_{15}$:
$(\mathsf{rhsp}' = \mathsf{rhsp} - 1) \wedge$
$(\mathsf{rmfp}' = \mathsf{rmfp} - 1) \wedge$
$(\mathsf{rhsp{:}\,rmfp}' = \mathsf{rhsp{:}\,rmfp} + 1);$

//HSP:MFP unbinding
$[]\ \mathsf{rhsp{:}\,rmfp} >= 1$
$\wedge\, \mathsf{rhsp} <= N - 1$
$\wedge\, \mathsf{rmfp} <= N_{PROT} - 1$
$\rightarrow \mathsf{rhsp{:}\,rmfp} * k_{16}$:
$(\mathsf{rhsp{:}\,rmfp}' = \mathsf{rhsp{:}\,rmfp} - 1)$
$\wedge(\mathsf{rhsp}' = \mathsf{rhsp} + 1)$
$\wedge(\mathsf{rmfp}' = \mathsf{rmfp} + 1);$

//Producing protein
$[]\ \mathsf{rhsp{:}\,rmfp} >= 1$
$\wedge\, \mathsf{rhsp} <= N - 1$
$\wedge\, \mathsf{rprot} <= N_{PROT} - 1$
$\rightarrow \mathsf{rhsp{:}\,rmfp} * k_{17}$:
$(\mathsf{rhsp{:}\,rmfp}' = \mathsf{rhsp{:}\,rmfp} - 1)$
$\wedge(\mathsf{rhsp}' = \mathsf{rhsp} + 1)$
$\wedge(\mathsf{rprot}' = \mathsf{rprot} + 1);$

Turku
Centre *for*
Computer
Science

Joukahaisenkatu 3-5 A, 20520 TURKU, Finland | www.tucs.fi

University of Turku
Faculty of Mathematics and Natural Sciences
- Department of Information Technology
- Department of Mathematics

Turku School of Economics
- Institute of Information Systems Sciences

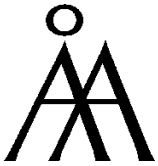

Åbo Akademi University
- Department of Computer Science
- Institute for Advanced Management Systems Research

ISBN 978-952-12-2622-9
ISSN 1239-1891